Earth-Science Reviews 249 (2024) 104664

Contents lists available at ScienceDirect

Earth-Science Reviews

journal homepage: www.elsevier.com/locate/earscirev

Invited Review

The past to unravel the future: Deoxygenation events in the geological archive and the anthropocene oxygen crisis

A.M. Mancini [a,*], F. Lozar [a], R. Gennari [a], R. Capozzi [b], C. Morigi [c], A. Negri [d]

[a] Earth Sciences Department, Università degli Studi di Torino, 10125 Torino, Italy
[b] Department of Biological, Geological and Environmental Sciences, Alma Mater Studiorum University of Bologna, 40126 Bologna, Italy
[c] Department of Earth Sciences, Università di Pisa, 56126 Pisa, Italy
[d] Department of Life and Environmental Science, Università Politecnica delle Marche, 60122 Ancona, Italy

ARTICLE INFO

Keywords:
Anoxia
Paleoenvironmental reconstruction
Dead zone
Climate change
Sapropel
Black shale
Hypoxia
Carbon cycle
Sediment

ABSTRACT

Despite the observation that we are witnessing a true oxygen crisis, the ocean deoxygenation theme is getting less attention from the media and population compared to other environmental stressors concerning climate change. The current ocean oxygen crisis is characterized by a complex interplay of climatic, biological, and oceanographic processes acting at different time scales. Earth system models offer insights into future deoxygenation events and their potential extent; however, their capacity to precisely constrain these events is complicated by the intricate interplay of various interconnected feedback mechanisms. The Earth's geological history has been punctuated by regional and global deoxygenation events, which are usually expressed by organic-rich sediment in the geological record and can be useful past analogues of the present-day and future oxygenation crisis related to current climatic stress.

Accordingly, we provide an overview of the key elements characterizing past deoxygenation events, aiming for a better understanding of the Anthropocene oxygen crisis and its potential evolution. We suggest that past global deoxygenation events during hypethermals may bear similarities to present-day dynamics in the open ocean. Additionally, we explore the significance of regional deoxygenation events with cyclical occurrences for better constraining environmental dynamics and ecological impacts in semi-enclosed, restricted, and marginal basins. Despite the unprecedented magnitude and rate of current anthropogenic pressures, it is essential to consider the comparison of triggers and feedbacks from ancient deoxygenation events when investigating the future of this concealed but ecologically impactful problem.

1. Introduction

Oxygen and life are tightly linked: the evolution and the proliferation of animals since ~600 Ma (Knoll and Carroll, 1999) was driven by the availability of molecular oxygen in the atmosphere and in the ocean. By contrast, oxygen depletion caused a biotic crisis of metazoans, as during the Permian-Triassic boundary event, when ~90% of marine species went extinct in a relatively short period (~61 ka) (Wignall and Hallam, 1992; Benton and Twitchett, 2003; Chen and Benton, 2012; Burgess et al., 2014).

Nowadays, climate change is altering global biogeochemical cycling and ecosystem health, including in the marine realm. Gruber (2011) described the modern ocean as "warming up, turning sour and losing breath" by accounting for the effects of warming, acidification, and deoxygenation. This "triple whammy" (Gruber, 2011) is the key stressor of marine ecosystems, which can create a negative synergic effect (Doney et al., 2012). Among the three key stressors, the alarming perturbations of the oxygen cycle (Limburg et al., 2020) is getting less attention from both science and society. This could be because deoxygenation often occurs in deep water or on the seafloor, in places hidden from the human eye. However, during the last 50 years, a global oxygen reduction of ~2% was recorded in the open ocean and in coastal areas, the latter characterized by the expansion of the so-called "dead zone" (Fig. 1) (Diaz and Rosenberg, 2008). Future projections suggest that under the Representative Concentration Pathways (RCPs) RCP8.5, approximately 100 Gt of O_2 would be removed from the atmosphere per year until 2100 (Huang et al., 2018).

The deoxygenation of seawater occurs when the oxygen is consumed

* Corresponding author.
E-mail address: alanmaria.mancini@unito.it (A.M. Mancini).

https://doi.org/10.1016/j.earscirev.2023.104664
Received 9 August 2023; Received in revised form 17 November 2023; Accepted 18 December 2023
Available online 26 December 2023

faster than its production or supply, and the degree of such deoxygenation can be established by threshold (expressed in milliliters of oxygen over a liter of marine water) indicating the quantity of dissolved oxygen in fluids. According to Tyson and Pearson (1991), marine water can be defined as anoxic (0 ml/l), suboxic (0–0.2 ml/l), dysoxic (0.2–2 ml/l) and oxic (> 8 ml/l) (Fig. 2). To define the level of oxygen at which biological and ecological processes are impaired, the term "hypoxic" is often used, and usually corresponds to 1.4 ml/l (Tyson and Pearson, 1991). However, this threshold may vary among taxa due to differences in oxygen requirements. For instance, many fishes and invertebrates experience hypoxia symptoms even at higher levels of oxygenation (Limburg et al., 2020). When deoxygenation conditions promote sulfate reduction, leading to the formation of hydrogen sulfide (H_2S), the water is defined as euxinic (Meyer and Kump, 2008).

The condition of oxygen starvation is known to slow down remineralization processes; hence, it represents an efficient pathway to preserve organic matter in sediments (Burdige, 2007). In fact, in the geological record, deoxygenation events are usually marked by distinctive "black" or "dark" layers, which are sediments characterized by the enrichment in organic carbon compared to the overlying and underlying sediments (Fig. 3). Depending on their spatial occurrences and the time interval in which they are deposited, these layers are either called "sapropel" (e.g., deposited in the Mediterranean during Neogene and Quaternary), "black shale" (e.g., during Mesozoic), "gyttjas" (e.g., deposited in the Baltic Sea), or simply "organic-rich layers". For simplicity hereinafter, we will refer to these layers as organic-rich sediment (ORS). ORSs have been extensively studied due to their economic significance as primary source rocks for oil and gas reservoirs. However, the deposition of ORS also plays a crucial role in carbon removal, acting as a significant sink for atmospheric CO_2 (Foster et al., 2018), as part of the biological pump (Sarmiento and Gruber, 2006). The ORS formed over broad geochronologic and geographic ranges, both during greenhouse periods (e.g., the Cretaceous Atlantic) and icehouse periods (e.g., the Pliocene–Pleistocene Mediterranean), at very different atmospheric pCO_2 levels (Negri et al., 2006). Enhanced organic carbon burial was either episodic or periodic during Earth's history depending on the trigger. Relatively short, single episodes were provoked by

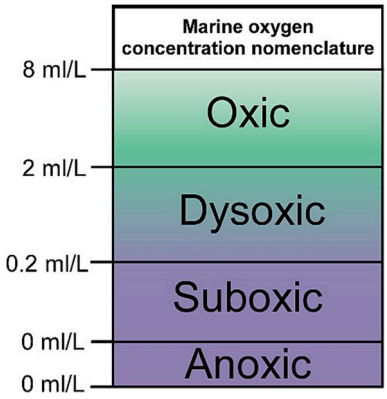

Fig. 2. Classification of marine environment based on the oxygen concentration. Modified after Tyson and Pearson (1991).

volcanic activity, but prolonged and periodic ORS deposition generally occurs when the climatic sensitivity of a sedimentary basin is increased due to the restriction of its oceanic gateways (e.g., Negri et al., 2006; Meyer and Kump, 2008; He et al., 2023). Coeval and globally distributed ORSs point to global anoxia in the deep environment, a situation without a modern equivalent; but regional ORS deposition in relatively shallow basins is also documented (Perissoratis and Piper, 1992; Sierro et al., 2003; Mancini et al., 2020), recalling dynamics occurring on present-day shelves (Mancini et al., 2023).

The ecosystemic response to deoxygenation is complex and hard to predict, mostly because of the non-linear sensitivity of organisms to oxygen starvation (Keeling et al., 2010) and for the resulting cascading effects on the food web (supplementary materials; Breitburg et al., 2015; Roman et al., 2019; Naqvi, 2020). As an example, a few simple organisms have evolved strategies to withstand oxygen depletion by using alternative electron acceptors, such as nitrate (denitrifiers) or other chemical species (sulfide or methane) (Aller, 2014). The complexity of climate change feedbacks acting at different time scales complicates the model build-up and the predictions of future scenarios (Oschlies et al.,

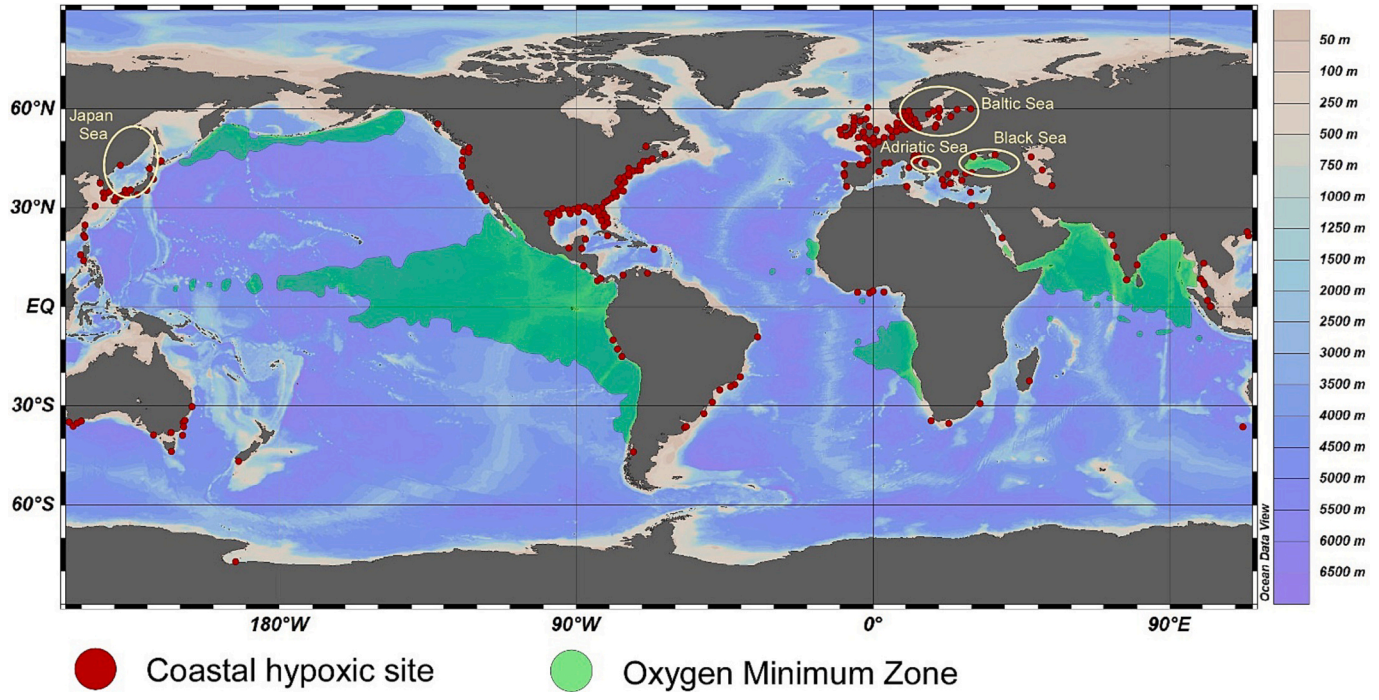

Fig. 1. Global map showing the coastal site affected by hypoxia and the Oxygen Minimum Zone at 300 m (<2 mg liter^{-1}). Data from Diaz and Rosenberg, 2008, updated by Breitburg et al. (2018). Map created with Ocean Data View software (Schlitzer, 2011; https://odv.awi.de, accessed on 2 December 2022).

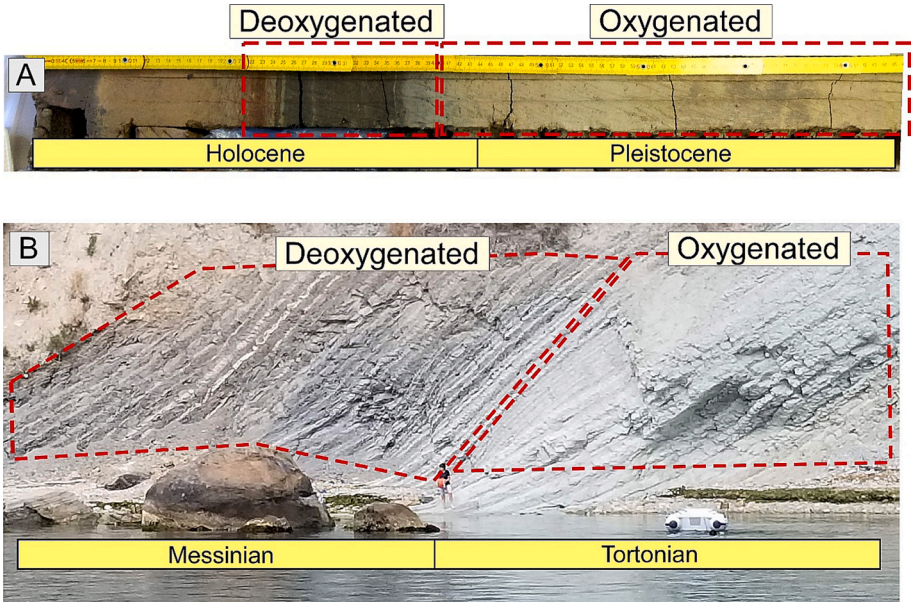

Fig. 3. Pictures showing the sedimentary expression of deoxygenation events. These events are usually marked by an increase in organic matter in the sediment, resulting in a darker coloration with respect to the overlying and underlying sediments.
A: The first meter of the core M25/4–12 recovered in the Ionian Sea (37°58′N 18°11′E) at 2467 m of water depth showing the most recent deoxygenation event (sapropel S1, ~10,000–6000 ya) in the deep setting of the Mediterranean. The core spans the last 27,000 ya.
B: Landscape view of the sedimentary expression of cyclical Messinian deoxygenation events outcropping in Ancona (central Italy 43°58′N 13°17′E). Note that each sedimentary cycle represents ~20,000 ya (Hilgen et al., 1995).
Yellow boxes indicate the geological stage in which the sediment was deposited.

2018; Foster et al., 2018). Nevertheless, the geological archive offers the opportunity to detail past deoxygenation events and constrain the ecosystem response to this kind of perturbation. Although environmental parameters can only be approximated by using proxies, the geological approach is a powerful tool to forecast future ecosystem changes under ongoing climate change, since it allows to address the mechanisms acting during past ocean deoxygenation events and provide the best and most plausible analogue for the current deoxygenation trend.

In light of this objective, we conduct a review of pivotal time

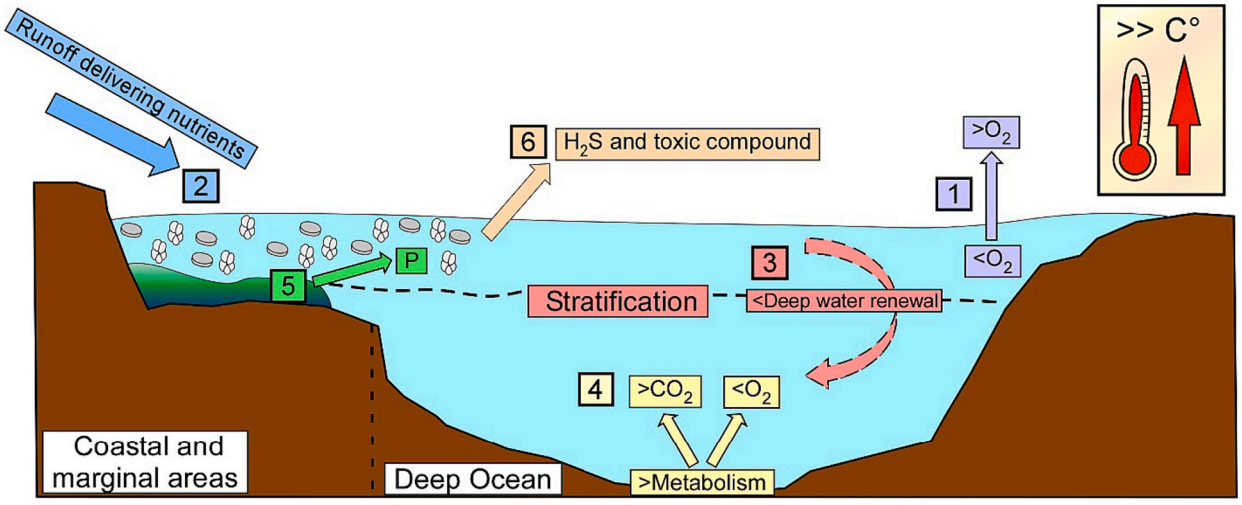

Fig. 4. Sketch showing the main biogeochemical and oceanographic changes related to deoxygenation in response to warming.
1: Reduction of oxygen solubility in seawater.
2: Increase in the hydrological cycle which increases the continental runoff. The nutrient delivery associated with freshwater input is enhanced by anthropogenic fertilization, thus promoting eutrophication and large organic carbon export to the seafloor which, once remineralized, consumes oxygen. The freshwater input carrying low-density water favour the stratification of the water column and increases the deoxygenation potential of bottom water.
3: Increase in thermal stratification, which hampers a correct deep-water renewal that provides oxygen to the Ocean interior.
4: Increase in metabolic consumption of oxygen by organisms.
5: The sediment beneath anoxic water releases phosphorus, which can act as positive feedback on initial deoxygenation by stimulating primary productivity. During anoxic conditions, sulfate reduction can promote the build-up of the toxic compound H_2S.
6: Increase in harmful algal bloom and associated toxic compounds.
The symbol < or > refers to a decrease or increase of the parameters, respectively.

intervals in Earth's geological history that exhibit deoxygenation dynamics. Our aim is to identify both similarities and differences between these periods and the ongoing deoxygenation pattern, thereby offering valuable insights into potential future trends. We also address prospective methodological improvements to further constrain our comprehension of past, current, and future deoxygenation dynamics.

2. Warming driving deoxygenation: process and feedback

Marine deoxygenation is related to the present-day ocean warming through different pathways: i) decreasing oxygen solubility in water; ii) reducing thermohaline circulation strength, and finally, iii) increasing metabolic consumption of oxygen by organisms (Keeling et al., 2010; Danovaro, 2018; Robinson, 2019) (Fig. 4). Additional forcing, such as human-induced eutrophication of coastal environment via river-delivered nutrients synergistically contribute to the oxygen loss (Diaz and Rosenberg, 2008) via remineralization of the organic matter by microbial respiration. Also, the warming is enhancing the hydrological cycle, which delivers more dissolved nutrients through continental runoff and therefore, increases the deoxygenation potential of the bottom water by increasing marine productivity. Increasing human-induced eutrophication is producing the expansion of the Oxygen Minimum Zones (OMZ) (Fig. 1) (Stramma et al., 2008; Keeling et al., 2010 and reference therein), which results from the remineralization of organic matter below the photic zone in eutrophic regions. Generally, the deoxygenation of the open ocean is mostly related to gas solubility, while in coastal areas the increased nutrient and organic matter loading linked with human activities is the dominant trigger (Breitburg et al., 2018; Pitcher et al., 2021). Surprisingly, also microplastic pollution can increase the deoxygenation of seawater as it can serve as substratum for fungi and bacteria, which degrade these compounds by consuming oxygen (Krueger et al., 2015). Without mitigation strategies, by the year 3000 around 3% of the total oceanic oxygen inventory (relative to 1960) is projected to be lost in relation to microplastic degradation (Kvale and Oschlies, 2023) and if this deoxygenation takes place in hypoxic environments, such as a dead zone or OMZ setting, the oxygen level could approach anoxic condition. In this regard, a detailed compilation of the modern deoxygenated environments and the related process is listed in the supplementary materials.

The complexity of understanding and forecasting future ecosystemic processes mostly resides in "Earth sensitivity", which is the response of the Earth system to an initial force. Therefore, understanding the feedback process that mostly contributes to Earth's sensitivity is necessary. The major positive feedback to deoxygenation dynamics is related to the build-up of phosphorus (P) (Meyer and Kump, 2008)(Fig. 4). Climate warming enhances the hydrological cycle, and consequently the weathering processes increasing the concentration of phosphorus in seawater. This promotes marine primary productivity, as PO_4^{3-} is the most limiting nutrient for marine primary production on geological time scale (Tyrrell, 1999). Under anoxic bottom conditions, nitrate is consumed by denitrifiers and the phosphorus is preferentially released from the sediment and diffused into the water column (Fig. 4) where it can further increase marine productivity, acting as positive feedback on the deoxygenation (Van Cappellen and Ingall, 1994; Handoh and Lenton, 2003; Meyers, 2007; Meyer and Kump, 2008; Watson et al., 2017). This mechanism is also referred as the "sediment-nutrient-oxygen feedback" (Filippelli et al., 2003), and is thought to play a major role in shaping ancient (Reershemius and Planavsky, 2021) and present-day deoxygenation dynamics (Eilola et al., 2009; Viktorsson et al., 2013; Reed et al., 2011; Pitcher et al., 2021).

Another feedback related to deoxygenation that can have negative effects on ecosystems by increasing mortality is the release of hydrogen sulfide (H_2S; Fig. 4) (Kump et al., 2005): during anoxic conditions, the sulfate reduction can promote the build-up of an H_2S reservoir according to the reaction:

$$2CH_2O + SO_4^{2-} \rightarrow H_2S + 2HCO_3^-.$$

H_2S is a toxic compound at concentrations as low as 4 μg l^{-1} (Smith et al., 1976), although selected bacteria, fungi or benthic foraminifera can withstand its presence (Mosch et al., 2012; Cardich et al., 2015; Glock et al., 2019). Also, harmful algal bloom and the associated release of toxic compounds typify eutrophic and hypoxic areas (Fig. 4) (Rabalais et al., 2009; Karlson et al., 2021).

3. The analogue conundrum

From a broader perspective, the geological record is the only means to establish background environmental parameters on a timescale predating 160 years ago, when consistent measurement of environmental parameters began in the research community. For example, the extended time series of Sea Surface Temperature (SST) dates back to 1854, but the reliability of the data is higher only after 1940 (Huang et al., 2017). Consequently, one of the most crucial roles of geoscientists is to contextualize the current ecosystem perturbations in relation to past geological events. However, the ongoing climatic processes are exceptional in terms of magnitude and rate, and the ability to recognize and describe past instances of significant environmental changes occurring in less than two hundred years depends on the achievable time resolution. In this regard, typical slow oceanic sedimentation rates limit the maximum resolution to the century/millennial scale, making it challenging to identify shorter events. Instead, areas with higher sediment and biogenic accumulations in high-productivity zones or inner shelf regions influenced by continental runoff (Hedges and Keil, 1995) prove to be more helpful. Numerous other factors further complicate the identification of past analogues and the reconstruction of the environment during those times, such as differences in paleogeography of the continents (Scotese, 2021), cryosphere, and biosphere (Foster et al., 2017). The distribution of continental masses, the location of oceanic gateways, and the presence of submerged physical barriers influence atmospheric and oceanic circulation patterns. Furthermore, shifts in primary producers, specifically between calcareous and siliceous organisms, have a significant impact on the biological carbon pump and its role in regulating climate and seafloor oxygenation (Bown et al., 2004; Tréguer et al., 2018). Nonetheless, the geological archive contains valuable information about the environmental response to forcing across different time scales, thereby enhancing our understanding of climate-ocean feedbacks (i.e., Earth sensitivity, see paragraph 2). In this regard, the geological reconstruction of past CO_2 and SST permitted estimating the warming caused by a doubling of atmospheric CO_2 (Sherwood et al., 2020; Lear et al., 2021). Furthermore, the geological record reveals "climate tipping points," which represent irreversible transitions from one climatic state to another (IPCC, 2019). Tipping points occur when changes in the climate system become self-perpetuating beyond or below a certain threshold. A modern example is the forecasted collapse of the Atlantic thermohaline circulation, which could occur within 50 ya at a global warming of 4 °C (Armstrong McKay et al., 2022). This will lead to an irreversible reorganization of the Asian and African monsoon systems and a southward shift in the Inter-Tropical Convergence Zone causing drying in Amazonia and Sahel regions and therefore reducing natural carbon sinks (Bozbiyik et al., 2011).

For instance, regarding deoxygenation, the geological record reveals that the transition from an oxic to an anoxic state in the Mediterranean deep water during the Holocene occurred rapidly (approximately 40 ya) (Marino et al., 2007). This transition has been attributed to a tipping point being exceeded, which has recently been suggested to be associated with the buildup of phosphorus in the sediment under reducing conditions (Hennekam et al., 2020). Therefore, despite the dissimilar rate of current climate change, studying such events provides valuable insights into Earth's sensitivity and tipping points related to deoxygenation.

4. Deoxygenation events in the geological record

Geological history has been punctuated by many examples of either widespread or regional anoxia (Fig. 5) that we describe in terms of causes and consequences. For this reason, we will treat separately the global anoxic events recorded through the Paleozoic, Mesozoic, and the regional anoxic events of the Cenozoic.

4.1. Oceanic anoxia associated with extreme global warming events (hyperthermal)

Paleozoic events such as the Late Cambrian Steptoean Positive Carbon Isotope Excursion (SPICE), the Late Ordovician – Early Silurian Hirnantian Ocean Anoxic Event (HOAE), and the Late Devonian Frasnian-Famennian (F—F) extinction events (Fig. 5), were characterized by widespread anoxia. Particularly, the HOAE and F—F (Fig. 5) exhibited extensive shelf and basin-wide anoxia, which coincided with mass extinctions (Wignall and Hallam, 1992; Bond et al., 2004; Boyer et al., 2014; Bond and Grasby, 2020; Pohl et al., 2021). The extinctions were associated with increased hydrogen sulfide in the water column or, as biomarker evidence suggests, gradual deoxygenation that depleted essential trace elements like Mo and Cu, resulting in marine productivity collapse and subsequent extinction (Anbar and Knoll, 2002; Bond and Grasby, 2020). These events occurred in a vastly different world from the modern one, not only due to different continental configurations and oceanic current regimes, but also distinct atmospheric oxygen concentrations (Lenton and Daines, 2017; Krause et al., 2018; Reershemius and Planavsky, 2021). Additionally, ancient sediments often underwent subduction, deformation, and erosion during multiple orogenic events, limiting paleoenvironmental investigations. Therefore, we will focus on better-constrained and extensively studied Mesozoic and Paleogene deoxygenation events, which are typically hyperthermal events.

These events share common features:

1- Emissions of greenhouse gases during prolonged continental or

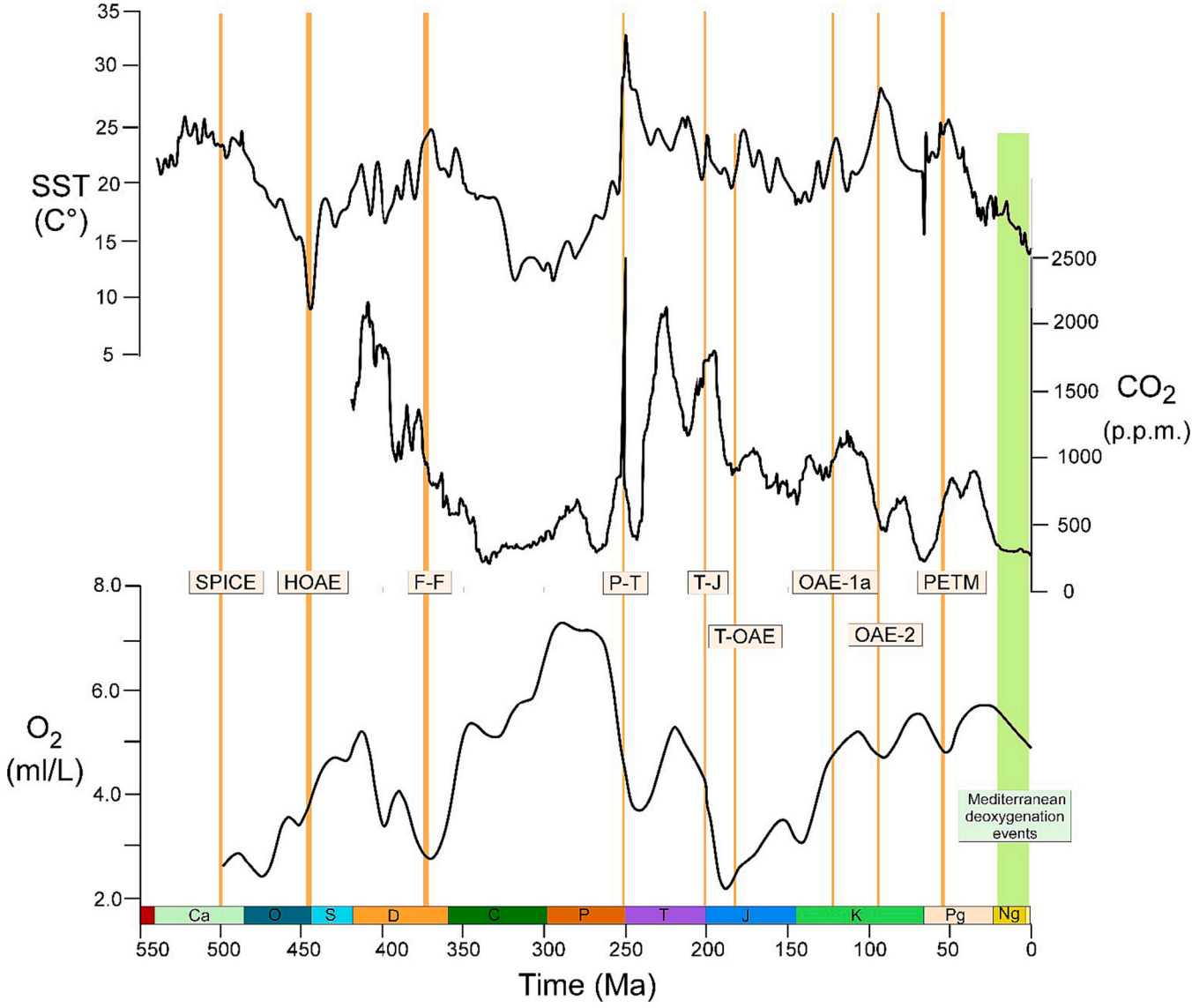

Fig. 5. Phanerozoic SST variation (Scotese et al., 2021) atmospheric CO_2 (locally estimated scatterplot smoothing best fit for all the different proxies applied; Foster et al., 2017 and Wu et al., 2021) and the dissolved oxygen in surface seawater (Song et al., 2019). The orange lines mark the timing of hyperthermal associated with major deoxygenation events (Meyer and Kump, 2008; Song et al., 2017; Song et al., 2019) (Permian-Triassic event, P-T; Triassic-Jurassic, T-J; Toarcian Oceanic Anoxic Event, T-OAE; Oceanic Anoxic Event, OAE-1a and OAE-2; Paleocene Eocene Thermal Maximum, PETM). Ca Cambrian, O Ordovician, S Silurian, D Devonian, C Carbonifererous, P Permian, T Triassic, J Jurassic, K Cretaceous, Pg Paleogene, Ng Neogene. *Re*-drawn from Foster et al. (2017), Song et al. (2019), Scotese et al. (2021) and Wu et al. (2021).

submarine volcanic activity (Ernst and Youbi, 2017; Foster et al., 2018; Hu et al., 2020).

2- Rapid warming associated with greenhouse gas (Arthur and Sageman, 1994; Meyer and Kump, 2008; Foster et al., 2018).

3- Duration exceeding 100 ka (Foster et al., 2018; Reershemius and Planavsky, 2021).

4- Sea level rise (Foster et al., 2018; He et al., 2023).

5- Deoxygenation (Arthur and Sageman, 1994; Jenkyns, 2010; Foster et al., 2018; Benton, 2018; He et al., 2023). This factor, combined with possible enhanced marine productivity, is responsible for the organic matter accumulation and for the enrichment of dolomite minerals in the sediment (Li et al., 2021).

6- Significant biotic response and/or biological reorganization (Leckie et al., 2002; Lowery et al., 2020). This often includes the reduction/disappearance of multicellular organisms and/or an increase in microbial bloom (Erba, 2004; Kuypers et al., 2004; van de Schootbrugge et al., 2007; Mays et al., 2021; Chen et al., 2023).

These hyperthermal events were also characterized by various feedback mechanisms, which can be summarized as follows:

a- Intensification of the hydrological cycle, leading to increased continental weathering and erosion, providing additional nutrients for phytoplankton growth and enhancing marine productivity (Arthur and Sageman, 1994; Meyer and Kump, 2008; Jenkyns, 2010). Such a process can act as positive feedback on marine deoxygenation (see paragraph 2) and can be particularly relevant in marginal seas and coastal areas (e.g., Elderbak et al., 2014; Lowery et al., 2018).

b- The runaway greenhouse effect, which involves a series of cascading effects that act as positive feedbacks on the initial input of greenhouse gases into the atmosphere. Following an initial greenhouse gas emission, the subsequent warming reduces the solubility of CO_2 in seawater, resulting in a net transfer from the ocean to the atmosphere. The warming also increases water evaporation and destabilizes methane gas hydrates, which are among the most potent greenhouse gases.

c- Organic carbon burial in sediment, which functions as negative feedback on greenhouse gas emissions (Jenkyns, 2018; Foster et al., 2018).

The magnitude of the impact associated with hyperthermals depended on factors such as the rate of greenhouse gas emission (constant rate vs. pulse), the nature of the emitted material (toxic vs. biolimiting), and the location of the primary emission source (submarine or terrestrial; latitude) (Leckie et al., 2002; Jenkyns, 2010; Ernst and Youbi, 2017; Lowery et al., 2020; Hu et al., 2020; He et al., 2023). Geodynamic processes drove the formation of Large Igneous Provinces (LIPs), which were responsible for the greenhouse gas emissions during hyperthermals. In general, terrestrial LIPs favoured rapid global warming, wildfires, climatic extremes (droughts and floods), the decline of carbonate platforms, ocean acidification and deoxygenation (Ernst and Youbi, 2017; Hu et al., 2020). On the other hand, submarine LIP emissions are generally characterized by elevated productivity fuelled by hydrothermal activities, OMZ development, deep-sea deoxygenation and marine plankton overturn (Leckie et al., 2002; Hu et al., 2020). The deoxygenation characterizing hyperthermal related to submarine LIP emission usually exerted a more pronounced impact on deep water settings compared to shallow marine and terrestrial settings (Hu et al., 2020), although the scarcity of open ocean and pelagic record limits the comprehension of the real extension and magnitude of deoxygenation (He et al., 2023).

One of the past global anoxic events that shares similarities with current and future climate change is the Permian-Triassic event (P-T, Fig. 5). This event took place 252 Ma and was responsible for the largest biotic crisis in geological history, resulting in the extinction of approximately 90% of marine and 75% of terrestrial species over a span of about 61 ka (Chen and Benton, 2012; Burgess et al., 2014). It took approximately 5 Ma for global taxonomic diversity to recover to pre-extinction values, and >50 Ma to restore the marine ecosystem structure (Song et al., 2018). There is a broad consensus that this catastrophic event was triggered by massive eruptions in what is now Siberia (Benton and Twitchett, 2003). These eruptions involved the submarine release of basaltic lava, covering an area equivalent to the European Union. Following an initial warming phase due to CO_2 emissions, gas hydrates and large volumes of methane were released into the atmosphere from the sediment (Retallack and Jahren, 2008; Sun et al., 2012; Benton and Twitchett, 2003; Benton, 2018; Joachimski et al., 2020; Wu et al., 2021; Wu et al., 2023), intensifying the greenhouse effect and resulting in a subsequent warming of approximately 8–10 °C (Joachimski et al., 2020). The atmospheric disturbance was transmitted to the oceans through two processes: i) the slowdown of deep circulation due to the reduced temperature gradient between latitudes, and ii) the reduced solubility of oxygen in warmer water (Wignall and Twitchett, 1996). The sluggish circulation led to deoxygenation, initially in deep waters and later in shallower shelf settings (Wignall and Twitchett, 1996). The Panthalassa Ocean likely remained euxinic for an extended period and remained anoxic until the beginning of the Middle Triassic, approximately 6 Ma after the onset of the disturbance (Isozaki, 1997). Ocean deoxygenation is considered the primary suspect trigger of this mass extinction event in the marine realm (Benton, 2018) due to its magnitude, duration, and expansion into shallow areas. For these reasons, this event is also known as the “superanoxic event” (Isozaki, 1994).

Later, in the Mesozoic (252–65 Ma), a series of abrupt oceanographic changes started to occur when the breakup of the supercontinents Gondwana and Pangea lead to the opening of the Atlantic Ocean to the West and the opening of the Tethys Ocean to the East, including the present-day Mediterranean area (Takashima et al., 2006). Known as Oceanic Anoxic Events (OAEs) and represented by ORSs in the sedimentary record, these are intervals related to major perturbations in the global carbon and oxygen cycle, at times even leading to euxinia throughout the water column and extinction events (He et al., 2023). The main ORSs having global occurrence are those related to the Triassic-Jurassic event (T-J, 201 Ma) T-OAE (Toarcian, 183 Ma), the OAE1a (Aptian, 120 Ma), and the OAE2 (Cenomanian/Turonian, 94 Ma) (Leckie et al., 2002; Takashima et al., 2006). Significant extinction rates of marine and terrestrial species, followed by diversification also characterize these events (Leckie et al., 2002; Erba et al., 2010; Rampino et al., 2019; Erba et al., 2019; Schoepfer et al., 2022).

The geodynamic restructuring observed during the OAEs coincided with the placement of LIP, such as the Central Atlantic Magmatic Province during the T-J and T-OAE at 201 Ma, the Ontong Java event at 120 Ma for OAE1a, and the Caribbean Plateau during OAE2 at 94 Ma. These events involved the release of substantial quantities of greenhouse gases (CO_2 and CH_4) at a rapid pace, intensifying the greenhouse effect and leading to a significant rise in global average temperatures (Bralower et al., 1997; Takashima et al., 2006; Scotese et al., 2021; He et al., 2023). The oceanic uptake of a fraction of the CO_2 emitted into the atmosphere also drove changes to the total alkalinity of seawater at all OAEs, shoaling the lysocline and the carbonate compensation depth (CCD) in the open ocean. Marine organisms with carbonate shells were the major target of the consequent biotic crisis (Erba, 1994; Leckie et al., 2002; Larson and Erba, 1999; Erba, 2004; Mattioli et al., 2009; Erba et al., 2010; Jones et al., 2023; Steuber et al., 2023).

In detail, the T-J event was characterized by shallow anoxia associated with a thermal-driven vertical expansion of the OMZ (Izumi et al., 2018), although some marine marginal sites remained well-oxygenated (Schoepfer et al., 2022). The geographic distribution of anoxia was also related to a long-term input of freshwater, which favoured the formation of a halocline and stratification, hindering an efficient thermohaline circulation (Jaraula et al., 2013). Due to its large biological reorganization, this event is usually ranked among the “big five” mass extinction events in the Earth history (Raup and Sepkoski, 1982; Bambach, 2006; Schoepfer et al., 2022).

The T-OAE (183 Ma) is characterized by greenhouse gas emissions from LIPs on the continent, which in turn caused global warming (7–10 °C) (Dera et al., 2011; Korte et al., 2015), and affected the

terrestrial and marine ecosystems with wildfires, droughts, acid rain, annihilation of carbonate platform, ocean acidification and deoxygenation, which collectively promoted extinction, turnover and migration of organisms (He et al., 2023). Conversely, OAE1a (120 Ma) and OAE2 (94 Ma) are characterized by greenhouse gas emissions from submarine LIPs (Bralower et al., 1997; Jenkyns, 2010); in these cases, major impacts affected the deep marine rather than the shallow marine or terrestrial environment. Noteworthy, bottom water anoxia was generally linked to water column stratification during OAE1a (Jenkyns, 2010), whereas OMZ expansion generally characterized OAE2 (Takashima et al., 2006) and led to a severe extinction of benthic organisms at shallow (carbonate platforms, e.g., Parente et al., 2008) and intermediate depth. These events were also characterized by eutrophication favoured by the formation of large shallow water marginal seas during new ocean opening, which are ideal site for nutrient traps and productivity enhancement (Trabucho Alexandre et al., 2010). This was accompanied by a reduction of sea-surface carbonate saturation, which disfavoured calcifying primary producers (Foster et al., 2018; Steuber et al., 2023) and, as in the case of T-OAE, it also drove dwarfism in the calcareous plankton and biomineralization crisis among benthic calcifying organisms (Steuber et al., 2023 and references therein).

Finally, the most recent global anoxic event is the so-called Paleocene Eocene Thermal Maximum (PETM) (56 Ma). The release of 1.1 Pg C ya^{-1} in ~4 ka due to volcanism that caused a rapid warming event (Zeebe et al., 2016), and the temperature rose by about 5–6 °C globally, accompanied by ocean acidification and deoxygenation, shallowing of the CCD, changing the hydrology and weathering regime and locally increasing primary productivity (Thomas and Shackleton, 1996; Zachos et al., 2005; Nunes and Norris, 2006; Carmichael et al., 2017; Bridgestock et al., 2019). In the continental shelf and restricted basins, where the marine productivity was enhanced (Tremolada et al., 2008), probably in response to the intensified runoff and chemical weathering (Robert and Kennett, 1994), the deoxygenation led to full anoxia and euxinic conditions (Speijer and Wagner, 2002; Sluijs et al., 2008; Nicolo et al., 2010; Carmichael et al., 2017). Furthermore, due to the increase in the hydrogen sulfide, the mesopelagic and bathypelagic zones became unhabitable by metazoans (Yao et al., 2018).

4.2. Regional deoxygenation events

Semi-enclosed basins like Japan, Mediterranean, Black and Baltic seas are preferentially hit by deoxygenation events because their circulation pattern and biogeochemical cycles are more sensitive to external forcings, such as those produced by climatic changes (e.g., continental runoff and nutrient input). Because of this they deserve more attention to interpret the current deoxygenation trends.

4.2.1. The Japan, Black and Baltic seas

Although largely oxygenated (excluding some cases, such as the Tokyo and Osaka bays), the Japan Sea experienced several deoxygenation events in its geological past. These were mostly related to the peculiar topographic configuration of this basin: the Japan Sea is a semi-enclosed and marginal basin surrounded by the Korean Peninsula, the Euroasian continent, and Japan island. Despite being a rather deep basin in its depocenter, the connection between the Japan Sea and the Pacific Ocean occurs through shallow sills present to the North-West and South-East at 130 m of water depth (Itaki, 2016). The interior of the modern Japan Sea is well-oxygenated due to the efficient thermohaline circulation, which can convey the oxygenated surface waters to the deeper seafloor through seasonal buoyancy loss (Talley et al., 2006), as occurring in the Mediterranean (Rohling et al., 2015). However, the basin experienced deoxygenation at intermediate and deep settings during both glacial and interglacial ages (Tada et al., 1999; Watanabe et al., 2007; Tada et al., 2015). Indeed, when the sea level drops during glacial periods, the Japan Sea lost the connection with the open ocean and therefore, was more influenced by continental runoff-driven stratification. In some cases, these deoxygenation events involved the entire water column up to the photic zone (Watanabe et al., 2007) and are lithologically expressed by sulfur-enriched ORS. Instead, thinner ORSs were deposited during interglacial periods in response to a complex oceanographic and climatic interplay between the coastal water of the East China Sea and the Japan Sea (Watanabe et al., 2007). Interglacial phases of the last 1.5 Ma favoured the influx of the East China low-salinity and nutrient-rich coastal water in the Japan Sea, promoting stratification and eutrophication and the consequent deoxygenation (Tada et al., 2018). Therefore, ORS deposits equally accumulate although in response to different conditions.

Shallow but large basins characterized by high freshwater input also suffer deoxygenation, as in the case of the brackish Baltic Sea. Here, the freshwater enters mainly from the northern area and the surface outflow occurs through the Danish strait to the North Sea. The density difference results in stratification of the water column separated by a halocline located at ~56 m. The semi-enclosed Baltic Sea is deserving particular attention because has, and is, suffering deoxygenation. The first record of hypoxia coincides with the transition from a freshwater to a brackish water body that occurred at 8000 ya in response to sea-level rise that connected the Baltic with the North Sea (Westman and Sohlenius, 1999). Successively, it experienced deoxygenation during the Medieval Climate Anomaly (200–750 ya BP) and during the last 115 ya, defined as modern hypoxic interval (Pitcher et al., 2021). The current deoxygenation in the coastal area of the Baltic Sea is severe, since 35% of the coastal systems experienced seasonal or episodic hypoxia in the period 1955–2009 (Conley et al., 2011). To note is that episodic hypoxia is considered a "precursor" of seasonal hypoxia (Conley et al., 2011). Deoxygenation is mostly related to enhanced nutrient delivery from agricultural land, which stimulates primary productivity, and by the warming (increase in stratification and respiration of O_2, and reducing O_2 solubility (Carstensen et al., 2014). The ORSs marking the present-day deoxygenation event in the Baltic Sea show Total Organic Carbon (TOC) values as high as 6% (Leipe et al., 2011; Leipe et al., 2017).

A similar situation is represented by the Black Sea, which during the Pleistocene was a freshwater lake; during Holocene sea level rise, the Mediterranean spill of marine water into the Black Sea caused the development of a permanent halocline, which promoted the creation of deep anoxic water. These processes were recorded by laminated ORSs dated ~3000–7000 ya (Giunta et al., 2007). In the modern setting, the Black Sea is the largest, deepest, and best example of anoxic and stratified basin (2200 m water depth) and below 100–150 m, it is euxinic and devoid of metazoan life (Tyson and Pearson, 1991).

4.2.2. The Mediterranean Sea

ORSs deposited in the Mediterranean Sea, a semi-enclosed basin connected to the Atlantic Ocean through a shallow and narrow sill at the Gibraltar Strait, have been extensively studied since their discovery following the Swedish Deep-Sea Expedition (1948).

The Western Mediterranean is separated from the Eastern part by the Sicily sill, resulting in different oceanographic circulation. The Eastern Mediterranean deep-water renewal and bottom oxygenation is provided by a fragile thermohaline circulation, driven by density gradients created by winter surface cooling and evaporation (Pinardi and Masetti, 2000). The Eastern Mediterranean bottom waters are trapped east of the Sicily Sill and are therefore more susceptible to deoxygenation. Differently, the Western Mediterranean can account for a more efficient bottom water oxygen renewal system, due to the Bernoulli aspiration acting in the Gibraltar Strait coupled with an effective deep oxygen renewal system acting near the Gulf of Lion (Rohling et al., 2015). The sedimentary record of the Eastern Mediterranean provided a succession of 88 distinct anoxic events regularly occurring during the last ~5 Ma (Emeis and et al., 1996). The older part of this record is also exposed in many inland successions and shows that ORS deposition also regularly occurred starting from the middle Miocene (Hilgen et al., 1995; Tayl-forth et al., 2014).

Noteworthy, although the Mediterranean ORS extends back to 15 Ma (Taylforth et al., 2014) most of the scientific effort was addressed to recent deep-sea ORS deposited in the eastern Mediterranean, namely, S1 (10 Ka) and S5 (124 Ka). Consequently, the general models proposed for the Mediterranean ORS deposition are based on studies on these better-constrained deposits (Rohling et al., 2015).

The relation between ORS deposition and climatic variation was pointed out by Parker (1958) and Emiliani (1955) and successively refined by Olausson (1961), ultimately allowing the tuning of the ORS with variation in the Earth's orbital parameters (Rossignol-Strick, 1983; Hilgen, 1991). Indeed, Mediterranean ORSs occur at minima of precession and maxima of insolation and are often considered the younger analogues of the Mesozoic ORSs, so Emeis and Weissert (2009) referred to the Mediterranean deoxygenation mode as a "mesocosm" for constraining the much older Mesozoic ORS deposition. This is because of the better-constrained stratigraphy and preservation of Mediterranean ORSs compared to the Mesozoic. Although the debate is still active, a general consensus exists regarding the primary role played by the climate-driven increase of freshwater input and SST in the Eastern Mediterranean (Castradori, 1993; Casford et al., 2002; De Lange et al., 2008; Rohling et al., 2015; Mojtahid et al., 2015; Blanchet et al., 2021; Mancini et al., 2023). At insolation maxima, not only the SST rise, but also the monsoon activity in Eastern Africa feeds the Eastern Mediterranean with a freshwater surplus which increased the surface water buoyancy (Rossignol-Strick, 1983). This mechanism increased the density gradient between upper and lower water masses, resulting in an almost permanent stratification and in the weakening or even stopping of the thermohaline circulation that provides oxygen to the seafloor. Additional freshwater sources, which contributed to diminishing the bottom oxygen renewal system through increased stratification were:

1) the increase in precipitation and runoff from the northern borderlands of the Eastern Mediterranean (Rossignol-Strick, 1987; Rossignol-Strick and Paterne, 1999; Rohling and Hilgen, 2007).

2) the Black-Sea outflow (Sperling et al., 2003; Rohling et al., 2015).

3) the sea level rise following warming towards insolation maxima (Rohling and Bryden, 1994; Rohling, 1994).

The increased freshwater input enhanced the deoxygenation potential through increasing primary productivity in two different pathways:

a) The river-delivered nutrients were responsible for the shift from the ultraoligotrophic Eastern Mediterranean region to a meso-eutrophic regime during the ORS deposition (Weldeab et al., 2014; Mojtahid et al., 2015; Blanchet et al., 2021). The primary productivity enhanced the organic carbon export to the sea bottom, which consumed oxygen through remineralization, favoring the preservation of organic matter in the sediment. This mechanism probably contributed to the development of most of the Quaternary ORSs in the Mediterranean (Emeis and Weissert, 2009).

b) A second mechanism is the formation of a Deep Chlorophyll Maximum (DCM), which is created when the pycnocline is located within the photic zone and divides an oligotrophic upper photic zone from a nutrient-replenished lower photic zone, stimulating the deep primary productivity. Despite the DCM production during ORS deposition is among the most recurrent feature recorded in paleoceanographic studies (Rohling and Gieskes, 1989; Castradori, 1993; Rohling et al., 2015), the relation between DCM production and anoxia is not completely understood. Some of the DCM autotrophs, referred as "shade flora" (Kemp et al., 2000), can create densely intricate mats that can bypass remineralization and zooplankton grazing processes by rapidly sinking to the seafloor (Brand et al., 2004; Pellegrino et al., 2018). These impenetrable structures hamper both epibenthic and infaunal activity, promoting the excellent preservation of seasonal laminae even in oxygenated environments (Brand et al., 2004; Pellegrino et al., 2020). Furthermore, the natural seasonal variation in the eastern Mediterranean oceanography, characterized by intense summer stratification with a fertile DCM, promoted a rapid settlement of the shade flora during autumn, when the cold-driven break-up of the stratification occurs. This phenomenon, referred to as "fall dump" (Fig. 6; Kemp et al., 2000), can greatly increase the export of organic carbon to the seafloor, promoting great oxygen consumption at the bottom.

4.2.2.1. The Western Mediterranean ORS. In the Western Mediterranean, the ORSs have lower TOC than in the Eastern Mediterranean, rarely exceeding 1.5% (Murat, 1999). These ORSs were deposited in response to deoxygenation down to anoxia (Rogerson et al., 2008; Pérez-Asensio et al., 2020) however, they are not always coeval with Eastern Mediterranean ORSs (Pierre et al., 1999; Murat, 1999; Rogerson et al., 2008), suggesting a different genetic mechanism. It was postulated that the Western Mediterranean ORSs were more likely linked to the high-latitude climatic and oceanographic changes, driving variation of the characteristic of the Atlantic inflow, able to modify the Western Mediterranean thermohaline circulation (von Grafenstein et al., 1999). Differently from its eastern counterpart, the western ORSs are less influenced by the continental runoff (especially from African rivers) and more by the sea-level rise and Sea Surface Salinity (SSS) drop, which can reduce the Bernoulli aspiration at the Gibraltar Strait and the surface water density, respectively (Rogerson et al., 2008; Rohling et al., 2015).

4.2.2.2. The Messinian and Pliocene ORS. Relatively few authors focused on ORSs pertaining to older time intervals, such as the Messinian and Pliocene, that instead show interesting features for our analysis. Regarding older ORSs, peculiar cases are those deposited on the shelf of the Sorbas basin (SW Spain) during the Messinian (7.16–5.97 Ma), which deserves a specific discussion. The Mediterranean paleogeography during the Messinian was similar to the modern one, although the gateways to the other bounding basins had different shapes (Flecker et al., 2015; Capella et al., 2019). Because of intense tectonic activity during this time, the uplift caused the progressive narrowing of the connection with the Atlantic, which proceeded by steps, dated at 7.1, 6.7, 6.4, 6.1 and 5.9 Ma (Sierro et al., 2003; Corbí et al., 2020; Mancini et al., 2020). This process promoted the restriction of the Mediterranean Basin and increased its susceptibility to climate and oceanographic variations. Indeed, the restriction step dated at 6.7 Ma decreased thermohaline circulation strength (increase in the deep-water residence time) and was responsible for the onset of the ORS deposition in the Sorbas Basin (Southeastern Spain, Sierro et al., 2003). According to Mancini et al. (2020), the inception of organic matter accumulation within sediments in the Sorbas Basin was triggered by an increase in organic carbon export under relatively eutrophic and cold conditions. Proxies reveal no signals of temperature increase, stratification, or DCM productivity, which typically characterize the onset of Quaternary ORSs (Mancini et al., 2023). One reason for this difference is the relatively shallow nature of the Sorbas ORS (100–200 m depth) compared to those in the Eastern Mediterranean (Mancini et al., 2023). In shelf environments, productivity and the export process play a crucial role in controlling bottom oxygen concentration and organic matter preservation in the sediment (Burdige, 2007; Mancini et al., 2020). The paleoenvironment of Sorbas bears similarities to modern OMZ settings (see supplementary materials), where oxygen deficiency is primarily driven by increased marine primary productivity.

During the Pliocene, the Mediterranean ORSs are particularly evident in the sedimentary record since the inception of the mid-Pliocene Warm Period (3.264–3.025 Ma) (Emeis and et al., 1996), when the global SST was 2.7–4.0 °C higher than today (Haywood et al., 2000; Haywood et al., 2013) and comparable with the SST predicted at the end of this century under the "business as usual" scenario (Lear et al., 2021). In this regard, the Pliocene ORSs may host precious information that can improve the understanding of the next future environmental dynamics related to deoxygenation. From 3.2 to 2.6 Ma, the ORSs were deposited in discrete coeval 'clusters' related to eccentricity maxima in Eastern Mediterranean deep-sea succession, which crop out also in land sections in Italian Apennines (Rohling et al., 2015). However, these

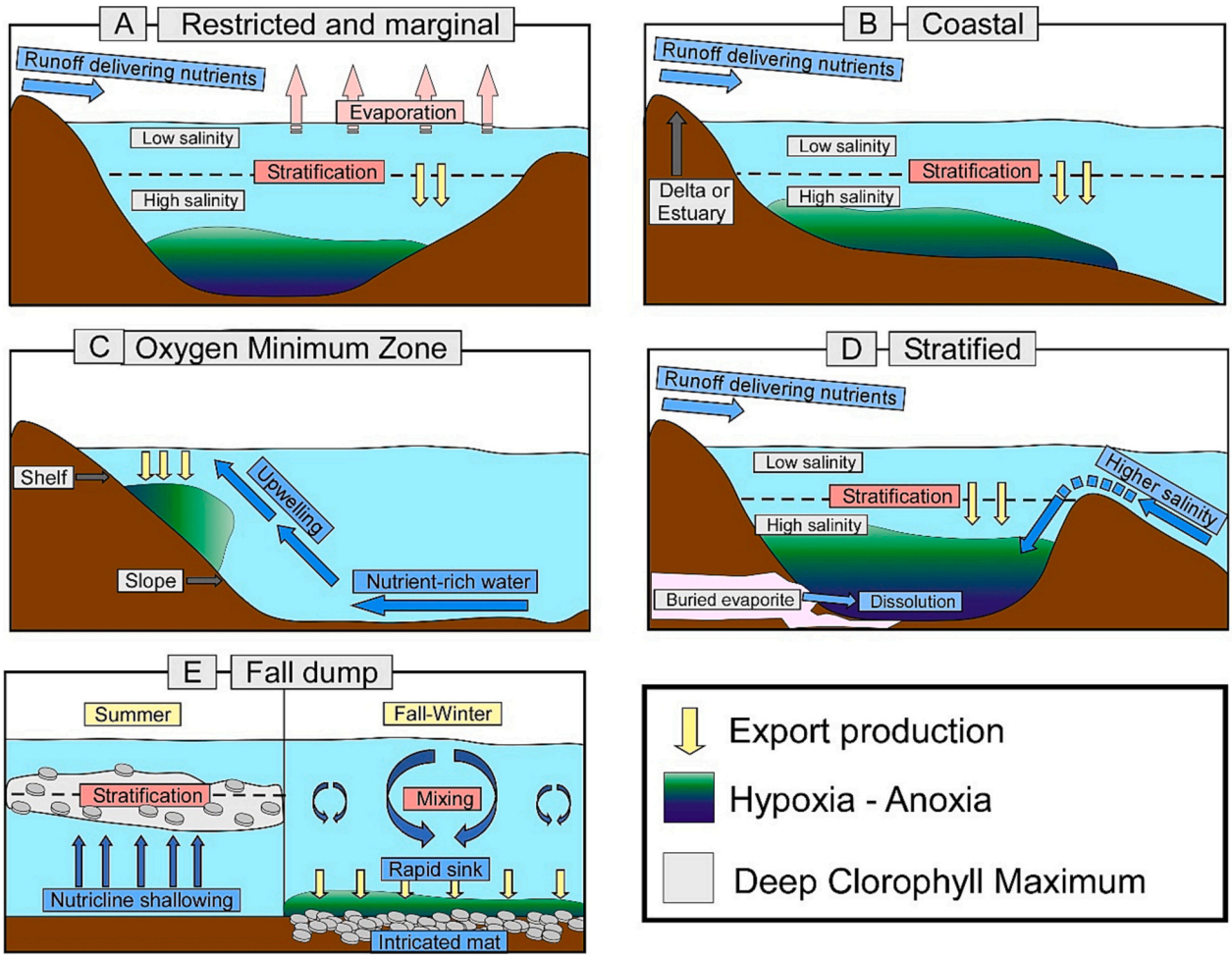

Fig. 6. Sketch showing the main environmental settings characterized by oxygen deficiency and related processes.
A: In restricted and marginal settings, such as lagoons, embayment or epicontinental seas, the freshwater influx and the evaporation flux result in a positive water balance, with low salinity water overlying more dense and salty water. The restricted exchange with the open Ocean and the nutrient delivery from land contribute to the oxygen deficiency at the bottom. Examples of this type of environment can be deep, as in the case of the Black Sea, or rather shallow, such as the marine karstic lakes of Mljet (42°47′ N, 17°21′ E; Adriatic Sea) (Wunsam et al., 1999; Sondi and Juračić, 2010) and the silled Etoliko lagoon (38°27′ N, 21°20′ S; Western Greece).
B: Coastal areas near river deltas or estuaries are subject to eutrophication, which can cause periodic or seasonal deoxygenation of bottom water. These environments are also under the influence of freshwater input, which can reduce the salinity in the upper water column, promoting a vertical stratification of the water column. Examples of this environment are the Chesapeake Bay (39°32′ N -76°04′ W; USA) and the Northern Adriatic in the Mediterranean.
C: High productivity setting with high carbon export are characterized by OMZ impingement at intermediate depth. These environments are usually characterized by the presence of nutrient-rich upwelling. Examples of this environment are the coasts of Perù, California and Arabian Sea.
D: Density stratification can result in permanent and/or sporadic deoxygenation of the seafloor. The density difference between the water masses can be provided either by saline water overspilling a physical sill, or by dissolution of buried evaporite at the bottom. Examples of this environment are the Baltic Sea (saline water overspilling the sill) or the Bannock Basin (Mediterranean Sea; Negri, 1996).
E: Organic carbon accumulation in the sediment and eventual deoxygenation (either confined at the sediment water interface or in the microenvironment surrounding the mats) is enhanced following the fall dump mechanism: During the warm season, thermal stratification of the water column occurs. If the surface water density is low enough to allow a shallowing of the nutricline inside the photic zone, high productivity confined in a DCM establishes. The DCM flora is usually composed by large diatoms, which can create an intricate mat inaccessible for the remineralization processes. During the recovery of the cooling-driving mixing process, the intricated biomass related to the DCM rapidly sinks to the seafloor, suppressing benthic activities and favoring organic carbon accumulation at the seafloor.

ORSs have also shelf equivalents, that provide information about coastal deoxygenation dynamics in a "warmer than today" Mediterranean. Most of the Pliocene shallow water ORSs were studied in on-land sections where they are finely laminated and deposited under a high sedimentation rate (3 to 6 cm/ka) (Capozzi et al., 2006a). Their organic carbon content mostly originated from marine organisms (Nijenhuis and De Lange, 2000; Capozzi et al., 2006a), suggesting enhanced primary productivity as the primary forcing for organic matter export to the sea floor. Furthermore, ORS records monospecific diatoms blooms (*Thalassiotrix–Thalassionema* group), alternated with oligospecific calcareous nannoplankton blooms (*Helicosphaera* group). According to Capozzi et al. (2006a, 2006b), the contribution of diatoms is particularly relevant among the primary producers, because their mats can increase the sinking rate of organic carbon (thus reducing the remineralization time), protect them from remineralization and can prevent bioturbation in seafloor surface sediments. This mode of ORS formation is particularly intriguing considering that the modern deoxygenation hotspots are linked to highly productive and coastal regions affected by eutrophication (Fig. 1). The increased organic carbon export and the peculiar aggregation style of the sinking organic matter may be related to the warm condition characterizing the Pliocene climate, responsible for the formation of a stable thermocline and the consequent DCM flora

proliferation. The biomass produced at depth then rapidly sunk to the bottom in response to cooling-driven mixing during late fall/early winter (i.e, "fall dump"), as suggested by Kemp et al. (2000).

All these Mediterranean examples show that a reduction of the thermohaline circulation through a decrease of the surface water density, coupled with an increase in organic carbon export are among the key factors controlling the bottom oxygen and therefore, the organic carbon stored in the sediment. Nevertheless, as outlined by Rohling et al. (2015): *there is not "one size fits all solution", ORSs will need to be considered individually, or perhaps in families, for their ecological characteristics.*

5. Analogies between modern and past records of deoxygenation and keys of interpretation

Our examination demonstrates the prevalence (and at times, ubiquity) of oceanic anoxia during certain periods in Earth's history (Canfield, 1998). However, due to thermohaline circulation and biogeochemical cycles, the modern oceans are predominantly oxygenated. In present-day environments, the occurrence of hypoxia is often linked to seasonal variations in productivity across numerous marine settings (Von Westernhagen and Dethlefsen, 1982; Seliger et al., 1985; Tyson and Pearson, 1991; Pitcher et al., 2021). Nonetheless, the areas most heavily impacted by deoxygenation are primarily marginal and/or silled basins (epicontinental seas), stratified basins, and upwelling zones (Fig. 6). Naturally, for a comprehensive reconstruction and interpretation of past deoxygenation events, it is imperative to leverage knowledge derived from contemporary environments. Additional information regarding these modern settings can be found in the supplementary materials, and a summarized overview is provided in Fig. 6.

From a wide perspective, the rapid greenhouse gas emissions related to volcanic activities that occurred during extreme events in the geological record can be regarded as a past analogue to the pulse of anthropogenic emissions that started with the industrial revolution. Human activities are now the major contributor to the perturbation of the carbon cycle: anthropogenic activities are hugely exceeding the greenhouse gas emission from volcanic activities, the latter corresponding to the CO_2 emission annually emitted in Florida (Gerlach, 2011). For example, during the P-T event, the reconstructed peak CO_2 emission was 0.7 Pg C ya^{-1}, which is 14 times lower than the current anthropogenic emissions of 9.9 Pg C ya^{-1} (Le Quéré et al., 2018; Jurikova et al., 2020). Similarly, the PETM, considered the largest carbon release event in the past 66 million years, was estimated to be nine times smaller (1.1 Pg C ya^{-1}; Zeebe et al., 2016) than the current emission rate. However, it is important to note that these hyperthermals occurred under significantly different conditions, with landmass distribution, ocean morphology, and ice cap extension profoundly different from today, making it challenging to directly compare the dynamics of the atmosphere and oceans. This implies that the modern and future CO_2 pulse cannot be simply equated with these hyperthermals. Instead, studying these events provides an opportunity to highlight ecosystem impacts and Earth sensitivity. For instance, the "runaway greenhouse" phenomenon observed during the P-T and other hyperthermal event is believed to have modern parallels (Lear et al., 2021). However, in the P-T event, the primary driver of the runaway greenhouse was the release of a significant amount of CO_2 into the atmosphere which increased the global temperature and promoted the melting of gas hydrates (Benton and Twitchett, 2003; Retallack and Jahren, 2008). While a substantial reservoir of gas hydrates (~500–2500 Gt of methane) exists in submarine environments today (Milkov, 2004), conclusive proof of methane hydrate reaching the atmosphere is still lacking (Ruppel and Kessler, 2017). Therefore, it seems that the methane gas hydrate feedback, at the moment, is not the most relevant feature characterizing modern climate change dynamics. Nonetheless, a considerable amount of methane is currently being anthropogenically emitted, especially in agriculture and waste, fossil fuel usage, biofuels, and biomass burning (Saunois et al., 2020). As a result, human activities are imitating the natural runaway greenhouse (i.e. destabilization of methane hydrates) processes observed during hyperthermal events. During these past extreme events, perturbations in the carbon cycles resulted in widespread deoxygenation, a situation that may be expected in our future.

An alarming parallel between the P-T event (and to a lesser extent, PETM and OAEs) and the modern era lies in mass extinctions. Although still debated (for detail see Briggs, 2016 and Cowie et al., 2022), the modern extinction rate over the past century is thought to be exceptionally high and falls within the range of past mass extinctions (Ceballos et al., 2015), suggesting that a sixth mass extinction is already underway due to human activities. Killing of the species, fragmentation of habitat, non-native species introduction, spreading pathogens and climate change are the main causes of the sixth mass extinction (Barnosky et al., 2011). The decline in biodiversity, driven by deoxygenation, is primarily associated with industrialization processes that began around 200 years ago in Europe and the USA and approximately 100 years ago in Asia (Rabalais et al., 2010; Yasuhara et al., 2017). Furthermore, it has been suggested that mass extinctions throughout the Phanerozoic occurred when a certain incremental temperature threshold of 5.2 °C above pre-event levels was exceeded within a relatively short time interval, at a rate exceeding 10 °C per million years (Song et al., 2021). Under the SSP5–8.5 emission scenario, this threshold is projected to be reached by approximately 2100 (Tebaldi et al., 2020; Song et al., 2021). During the P-T event, the primary killing mechanism responsible for the mass extinction in the marine realm was a combination of deoxygenation and lethal heating (Song et al., 2014; Penn et al., 2018; Benton, 2018). This bears some similarity to what is observed in modern settings, where heatwaves and eutrophication reduce oxygen solubility and increase mortality (Brauko et al., 2020; Limburg et al., 2020). If these impacts affect areas hosting endemic species, species extinction becomes highly probable. Additionally, the cascading effects of deoxygenation on the trophic web can diminish biodiversity and raise the potential for species extinction. Persistent organic pollutants also contribute to deoxygenation-driven mass mortality, particularly in marine pollution hotspots like the Mediterranean and the northwestern European coast (Handoh and Kawai, 2014). The current mass mortality observed in hypoxic-anoxic zones may foreshadow more severe and widespread effects in the future, especially if warming affects eutrophic areas.

Furthermore, the terrestrial or submarine location of the primary greenhouse gas emissions is a crucial factor influencing the magnitude and spatial distribution of deoxygenation (refer to paragraph 4.1) and mass extinction. As modern greenhouse gas emissions are mostly derived from terrestrial sources, we can expect a stronger impact of deoxygenation on shallow and marginal sea ecosystems compared to the open ocean and deep sea. This is indeed observed in the modern oceans (Fig. 6; Diaz and Rosenberg, 2008; Breitburg et al., 2018; Brauko et al., 2020), primarily attributed to the accelerated hydrological cycle and human-induced eutrophication. However, from a geological perspective, if warming continues, there is a likelihood of widespread or even global deoxygenation similar to the events observed during hyperthermal periods. This probability arises mainly due to decreased oxygen solubility, increased water stratification in the open ocean and enhanced oxygen demand by organisms.

To identify comparable situations to the current conditions in the enclosed and coastal areas affected by fertilizer-enriched runoff, leading to eutrophication and deoxygenation (Fig. 6B), and their significant impact on ecosystem functioning (Breitburg et al., 2018), it is necessary to examine the Messinian ORS deposited in Sorbas Basin. As reported in paragraph 4.2, the deposition of these ORSs was initially triggered by increased marine productivity and organic carbon export to the bottom in a relatively cold context, promoting intermittent oxygen deficiency. This condition represents an analogue of the modern situation in several enclosed, marginal and coastal areas, such as the Chesapeake and Osaka bays and the Northern Adriatic (Fig. 6B), where seasonal productivity

peaks and stratification contribute to deoxygenation pulse (Fig. 5; Stachowitsch, 1984; Crema et al., 1991; Kemp et al., 2005; Stachowitsch et al., 2012; Yasuhara et al., 2019). For instance, in the modern Northern Adriatic, the nutrient-delivered eutrophication caused transient events of bottom deoxygenation with large mortalities of benthic organisms (Crema et al., 1991); these events are increasing in both magnitude and frequency (Penna et al., 2004; Stachowitsch et al., 2012). To give an idea of the magnitude, in September 1983 in the Gulf of Trieste (Northern Adriatic), 90% of the total epifaunal biomass died within 2 days in response to deoxygenation over an area of ~250 km^2 (Stachowitsch, 1984). In the Sorbas Basin ORS, permanent anoxic conditions were reached in response to increasing freshwater input and temperature; the SST variation calculated (~ 0.001 °C $year^{-1}$) occurred over 10 Ka (Mancini et al., 2023). This SST changes was one order of magnitude slower than the warming rate measured in the Mediterranean in the 1986–2015 interval (i.e., 0.04 °C $year^{-1}$), and two orders of magnitude slower than the projected warming in the 2071–2100 interval (i.e., 0.68 °C $year^{-1}$) (Sakalli, 2017; Mancini et al., 2023). This suggests that the ongoing warming, which is occurring at a faster and more intense rate compared to the conditions that caused anoxia in the Messinian period, is likely to result in more extensive and severe deoxygenation in these marginal environments.

Another intriguing example pertains to the Pliocene ORS found in the Northern Apennine region of Italy. These sediments were formed during a period that was warmer than the present era (Haywood et al., 2000; Haywood et al., 2013; Lear et al., 2021). In response to heightened primary productivity, these deposits exhibit distinctive characteristics in the way organic matter settles, primarily comprised of intricate diatom mats. This intricate settling pattern facilitated rapid sinking, leading to bottom deoxygenation and enhanced preservation of organic carbon within the sediment. As the Pliocene ORSs are interpreted as triggered by eutrophication during warm conditions (Capozzi et al., 2006a), they suggest that future deoxygenation dynamics might be focused in highly productive and warm regions, corresponding to the settings reported in Fig. 6A, B and C. Noteworthy, diatoms account for ~40% of the primary productivity and export in the ocean (Tréguer et al., 2018) and are characterized by a higher growth rate compared to other phytoplankton groups (Kemp and Villareal, 2018). Some diatoms taxa are able to bloom confined in a DCM, a structure that can be related to warming-driven stratification. The DCM structure is hidden from the satellite observation of primary productivity, which can detect only the uppermost few meters of the water column. Therefore, the assessment of the primary production confined in a DCM necessarily comes from in situ observation. For instance, in the Southern Ocean, the diatom-dominated DCM constitutes up to 50% of the total water column production (Parslow et al., 2001; Gomi et al., 2010). Under climatic warming, the stratification of the water column is enhanced and an increase in diatom inhabiting the DCM is expected in the coming years acting as negative feedback on the CO_2 because of the increasing carbon export and burial (Kemp and Villareal, 2013). Also, the increasing warming-driven stratification will likely enhance the full dump process, with negative repercussions on the bottom oxygen inventory. The Pliocene ORSs recorded in the Northern Apennine teach us that under warmer conditions than today, the phytoplankton has responded by changing its composition, properties, and spatial distribution, resulting in an increase in carbon export to the sea bottom, which promotes deoxygenation. Similar to the Messinian ORS of Sorbas, these layers were deposited in shallow environments (Capozzi et al., 2006a), where productivity and export processes play a pivotal role in controlling the bottom oxygen budget (Fig. 6A and B). Hence, we strengthen the need to delve deeper into the comprehension of this sedimentary record as they can provide significant clues in understanding the present issues. Also, the detailed reconstruction of the mechanisms regarding the onset and recovery of these shallow sea ORSs can significantly contribute to develop effective strategies for the mitigation of the risk associated with the expanding hypoxic regions.

Instead, the deep Eastern Mediterranean Sea Quaternary ORS deposits originate from weakening or cessation of the thermohaline circulation, which supplies oxygen to the seafloor (De Lange et al., 2008; Rohling et al., 2015) (setting reported in Fig. 6A). Consequently, they serve as a warning about the potential occurrence of deep-sea anoxia. However, recent studies investigating the contemporary behavior of the thermohaline circulation indicate that although its strength is diminishing (Somot et al., 2006), the Eastern Mediterranean is projected to maintain adequate oxygenation levels throughout the next century (Powley et al., 2016). This is mostly because, in contrast to what happens during events of deep-water stagnation and ORS deposition, the Mediterranean is characterized by a drying trend (Sanchez-Gomez et al., 2009), which counteracts the density loss of surface water provided by warming, hence promoting deep convection. Additionally, the continental runoff from the Nile River, which is considered the main freshwater input source during ORS formation, almost stopped after the building of the Aswan High Dam (Rohling and Bryden, 1992). All in all, the environmental changes associated with the deep-sea Mediterranean ORS cannot compare to the current (and predicted) environmental setting (Mancini et al., 2023). Nonetheless, they can provide as well important clues on the rate at which the deoxygenation process proceeds. In this regard, the study of the most recent and best age-constrained ORS deposited in the Eastern Mediterranean (i.e., sapropel S1) allowed to unravel the time involved in the transition from oxic to anoxic state and vice versa, that in the Aegean Sea, occurred in ~40 ya (Marino et al., 2007). Other information comes from a cold episode in the northern borderland dated at 8.2 ka that resulted in a resumption of the deep thermohaline circulation leading to sudden oxygenation, usually marking the S1 interruption (Rohling et al., 2015; De Lange et al., 2008; Filippidi and De Lange, 2019). All these relatively fast transitions of bottom oxygen levels highlight the Mediterranean thermohaline circulation sensitivity to climatic and oceanographic changes. However, the deoxygenation dynamics during the Quaternary characterizing the coastal and shallow environment were less constrained than the deeper counterpart, despite these areas in the present-day settings (Fig. 6B) are more influenced by oxygen depletion in the Mediterranean (Capozzi and Negri, 2009), providing evidence for the need to deepen this kind of investigation.

To conclude this review, it is crucial to emphasize the significance of the Baltic Sea as a pivotal case, which is considered the largest anthropogenically-induced hypoxic zone in the world (Conley et al., 2009), in which ORSs are currently depositing and may offer the opportunity to highlight the ecosystem impact related to deoxygenation. The Baltic Sea deoxygenation dynamics were (and are) strongly linked with warming periods, making this environment a deoxygenation hot spot for the near future. The mixing of bottom hypoxic water with surface water can cause harmful algal blooms associated with the mortality of shellfishes, fishes, and occasionally dogs (Rose et al., 2019; Karlson et al., 2021). In the Danish Straits of the Baltic Sea in 2002, a large event of seasonal hypoxia is thought to have killed 300,000 tons of benthic fauna, which is almost equivalent to the Danish human population (Carstensen and Conley, 2019). Such impact on benthic organisms represents further positive feedback on deoxygenation, preventing nutrient removal by the benthic biocenosis (Carstensen and Conley, 2019). The deoxygenation of Baltic Sea is an example of the impact on the economy of the bordering countries, which are reducing the quality and amount of caught fish (Rose et al., 2019). What is more important, is that in restricted and marginal areas undergoing anthropogenically induced eutrophication, deoxygenation can be reversed with persistent efforts addressed to reduce nutrient loading (Diaz and Rosenberg, 2008; Rabalais et al., 2010), mostly through wastewater treatment, wetland restoration, and management-mitigation strategies (Brauko et al., 2020). This is also illustrated by the recovery from coastal hypoxia in the Black Sea after the slowdown of agricultural and industrial activities in 1990 (Mee, 2006). Therefore, these two cases shed some hope on the possibility to mitigate this risk, but the recovery process from hypoxia

takes more time than its development, and typically involves a decadal timescale (Steckbauer et al., 2011), consequently pointing to urgent management strategies to face the current oxygen crisis. Also, the Baltic area may represent the "missing link" connecting the past to the present era; deepening the sedimentological study of this area by having at disposal archeological and modern data permit to understand the deoxygenation processes and help to counteract their effect.

6. Perspective

In our review, we present evidence of how combining a geological perspective with knowledge of the modern environment can contribute to understanding our future. Geological data play a crucial role in building and validating climate projections. Now more than ever, climate models require a vast amount of data to accurately constrain environmental dynamics related to climate change. Studying the past is essential for establishing baseline conditions, evaluating tipping points, assessing ecosystem repercussions, and understanding the recovery dynamics of ecosystems.

However, there are two main challenges in using the geological record to predict future changes: time resolution and quantitative parametrization of environmental variables. The first challenge arises from the different time scales observed by scientists from various disciplines, such as geology and biology. Biologists often provide highly accurate snapshots, but they cannot rely on long time series, whereas geologists focus on long time scales, sometimes spanning millions of years. This disparity arises because the sedimentary resolution is intricately linked to sedimentation rates, which often limit paleoenvironmental resolution at smaller time scales. The "meeting point" of these two investigation strategies can be found in laminated sediments. These sediments are primarily deposited under oxygen-depleted conditions, impeding bioturbation by organisms and preserving undisturbed laminae. These laminae often record biogeochemical and oceanographic changes related to seasonal variations, enabling paleoenvironmental reconstructions at the seasonal scale (Schimmelmann et al., 2016). Achieving seasonal resolution in paleoceanographic studies in a routinary way would bridge the gap between short historical series obtained through regular observations in modern environments, and the long-term proxy-based reconstructions provided by the geological record. Additionally, reconstructing past interannual variability through lamina-scale analysis is crucial for understanding patterns of modern short-lived anomalies, such as rapid deoxygenation events or heatwaves.

The second challenge lies in quantitatively parameterizing environmental variables using absolute values, which are essential for data assimilation in model-based studies. The study of the past heavily relies on proxies, which often provide qualitative indications that may not be easily translated into quantitative parameters. This limitation stems from the nature of proxies, which often require numerous assumptions for the quantitative conversion of observations and analyses from rock samples. However, there are emerging proxies capable of providing reliable quantification of past oxygen concentrations. For instance, transfer functions are now available to convert geochemical properties (e.g., authigenic uranium in sediments; Hu et al., 2023) or fossil features (e.g., benthic foraminiferal assemblages; Kranner et al., 2022) into quantitative oxygen content (for more information on paleoredox proxies, refer to the supplementary materials). These approaches should be favoured to enhance the production of quantitative data for model-based analyses and ultimately improve our understanding of past, present, and future deoxygenation dynamics.

Hence, it is crucial to recognize the significance of studying the past in conjunction with other applied methodologies and observations, which form most deoxygenation studies. Integrating insights from the past can enhance our understanding of this phenomenon, providing valuable perspectives to the existing body of research.

7. Conclusion

In the geological past, the deoxygenation of marine water occurred either stochastically (e.g., volcanism) and/or cyclically (e.g., variation in Earth orbital parameters); some of these events may provide valuable information for our understanding of current and future deoxygenation dynamics under climatic alteration. Our analysis of the geological record indicates that anthropogenic greenhouse gas emissions far exceed those associated with major and highly lethal deoxygenation events in the past, such as during the P-T mass extinction. Additionally, the rate of warming observed during past hyperthermals is dwarfed by the current rate of warming. A worrisome parallel can be drawn between the current extinction rate and the extinction event during the P-T, even though the underlying causes diverge.

The most recent Quaternary deep-sea ORS deposits in the Eastern Mediterranean, despite being extensively studied, do not provide the best analogue for understanding current and future deoxygenation dynamics in this region. This is because the climatic (warming and drying) and oceanographic conditions (construction of the Aswan High Dam) are not comparable. Instead, the often-overlooked ORS deposits in shallow settings, which occurred under conditions similar to the present, may hold the key to better understanding the dynamics of current and future deoxygenation in coastal areas, which are currently experiencing the greatest impact. Specifically, the Messinian ORS deposits in the Western Mediterranean, within a small and restricted basin, exhibit organic carbon accumulation in response to eutrophication, similar to what is observed in modern sea settings. Based on the dynamics of Messinian ORSs, further deoxygenation can be expected if warming continues to affect eutrophicated areas. Furthermore, the deposition of Pliocene ORS in shallow settings of the Adriatic Basin, resulting from heightened productivity and export to the seafloor, primarily facilitated by the exceptional aggregation of diatom mats, holds potential insights into future processes that may occur when SST reaches Pliocene levels, expected to occur by 2100.

Our analysis leads to the conclusion that the rapid rate of modern climate warming, whose magnitude exceeds all the past hyperthermals, is causing the deoxygenation of marine waters comparable to the onset of past regional deoxygenation events (as observed in ORS deposits in shelf settings). Without effective mitigation strategies, there is a possibility that in the future, the magnitude and spatial extent of ancient deoxygenation events may be surpassed, as anthropogenic activities are accelerating the natural pace of the runaway greenhouse effect characteristic of hyperthermal events.

It is important to keep in mind that even if greenhouse gas emissions were to immediately cease, warming would continue as the carbon cycle would require many years to recover to pre-industrialization levels. However, deoxygenation in marginal and coastal environments can be reversed if mitigation strategies are applied, as demonstrated by the Baltic and Black seas cases. Therefore, the geological perspective provides clues for better understanding and constraining the deoxygenation issue and its related impacts at different time scales. Also, we identify some aspects that may need to be improved for better constraining the deoxygenation issue and its related impacts, such as an improvement of the quantitative observation and the comparison of the analysed time scale. Our analysis reinforces the pivotal role of Earth science research in understanding the mechanisms responsible for past widespread or regional events, thus enabling a better understanding of the timing involved in the process and distinguishing the anthropogenic role in current global changes. This is crucial to help stakeholders and administrators to take the most effective measures to mitigate the risks.

Declaration of Competing Interest

The authors declare no conflict of interest.

Data availability

No data was used for the research described in the article.

Acknowledgements

This project was supported by CRT (Cassa Risparmio Torino) grant 2021.0907 awarded to Francesca Lozar

Appendix A. Supplementary data

Supplementary data to this article can be found online at https://doi.org/10.1016/j.earscirev.2023.104664.

References

Alexandre, Trabucho, et al., 2010. The mid-Cretaceous North Atlantic nutrient trap: Black shales and OAEs. Paleoceanogr. 25 https://doi.org/10.1029/2010PA001925. PA4201.

Aller, R.C., 2014. Sedimentary diagenesis, depositional environments, and benthic fluxes. In: Holland, H.D., Turekian, K.K. (Eds.), Treatise on Geochemistry, , Second editionVol. 8. Elsevier, Oxford, pp. 293–334.

Anbar, A.D., Knoll, A.H., 2002. Proterozoic Ocean chemistry and evolution: a bioinorganic bridge? Science 297, 1137–1142.

Armstrong McKay, D.I., et al., 2022. Exceeding 1.5 C global warming could trigger multiple climate tipping points. Science 377 (eabn7950). https://doi.org/10.1126/science.abn7950.

Arthur, M.A., Sageman, B.B., 1994. Marine black shales: depositional mechanisms and environments of ancient deposits. Annu. Rev. Earth Planet. Sci. 22, 499–551.

Bambach, R.K., 2006. Phanerozoic biodiversity mass extinctions. Annu. Rev. Earth Planet. Sci. 34, 127–155.

Barnosky, A.D., et al., 2011. Has the Earth's sixth mass extinction already arrived? Nature 471, 51–57.

Benton, M.J., 2018. Hyperthermal-driven mass extinctions: Killing models during the Permian–Triassic mass extinction. Phil. Trans. R. Soc. A 376, 20170076, 2130.

Benton, M.J., Twitchett, R.J., 2003. How to kill (almost) all life: the end-Permian extinction event. Trends Ecol. Evol. 18, 358–365.

Blanchet, C.L., et al., 2021. Deoxygenation dynamics on the western Nile deep-sea fan during sapropel S1 from seasonal to millennial timescales. Clim. Past 17, 1025–1050.

Bond, D.P., Grasby, S.E., 2020. Late Ordovician mass extinction caused by volcanism, warming, and anoxia, not cooling and glaciation. Geology 48, 777–781.

Bond, D., Wignall, P.B., Racki, G., 2004. Extent and duration of marine anoxia during the Frasnian–Famennian (Late Devonian) mass extinction in Poland, Germany, Austria and France. Geol. Mag. 141, 173–193.

Bown, P.R., Lees, J.A., Young, J.R., 2004. Calcareous nannoplankton evolution and diversity through time. In: Thierstein, Hans R., Young, Jeremy R. (Eds.), Coccolithophores: From Molecular Processes to Global Impact. Springer, pp. 481–508.

Boyer, D.L., Haddad, E.E., Seeger, E.S., 2014. The last gasp: trace fossils track deoxygenation leading into the Frasnian–Famennian extinction event. Palaios 29 (12), 646–651.

Bozbiyik, A., Steinacher, M., Joos, F., Stocker, T.F., Menviel, L., 2011. Fingerprints of changes in the terrestrial carbon cycle in response to large reorganizations in ocean circulation. Clim. Past 7, 319–338.

Bralower, T.J., Fullagar, P.D., Paull, C.K., Dwyer, G.S., Leckie, R.M., 1997. Mid-Cretaceous strontium-isotope stratigraphy of deep-sea sections. GSA Bull. 109, 1421–1442.

Brand, L.R., Esperante, R., Chadwick, A.V., Poma Porras, O., Alomía, M., 2004. Fossil whale preservation implies high diatom accumulation rate in the Miocene-Pliocene Pisco Formation of Peru. Geology 32, 165–168.

Brauko, K.M., et al., 2020. Marine heatwaves, sewage and eutrophication combine to trigger deoxygenation and biodiversity loss: a SW Atlantic case study. Front. Mar. Sci. 7, 590258. https://doi.org/10.3389/fmars.2020.590258.

Breitburg, D.L., et al., 2015. And on top of all that… Coping with ocean acidification in the midst of many stressors. Oceanography 28, 48–61.

Breitburg, D., et al., 2018. Declining oxygen in the global ocean and coastal waters. Science 359, eaam7240.

Bridgestock, L., Hsieh, Y.T., Porcelli, D., Henderson, G.M., 2019. Increased export production during recovery from the Paleocene–Eocene thermal maximum constrained by sedimentary Ba isotopes. Earth Planet. Sci. Lett. 510, 53–63.

Briggs, J.C., 2016. Global biodiversity loss: exaggerated versus realistic estimates. Environm. Skept. Crit. 5, 20.

Burdige, D.J., 2007. Preservation of organic matter in marine sediments: controls, mechanisms, and an imbalance in sediment organic carbon budgets? Chem. Rev. 107, 467–485.

Burgess, S.D., Bowring, S., Shen, S.Z., 2014. High-precision timeline for Earth's most severe extinction. PNAS 111, 3316–3321.

Canfield, D.E., 1998. A new model for Proterozoic ocean chemistry. Nature 396, 450–453.

Capella, W., et al., 2019. Mediterranean isolation preconditioning the Earth System for late Miocene climate cooling. Sci. Rep. 9, 3795.

Capozzi, R., Negri, A., 2009. Role of sea-level forced sedimentary processes on the distribution of organic carbon-rich marine sediments: a review of the late Quaternary sapropels in the Mediterranean Sea. Palaeogeogr. Palaeoclimatol. Palaeoecol. 273, 249–257.

Capozzi, R., Negri, A., Picotti, V., Dinelli, E., Giunta, S., et al., 2006a. Mid-Pliocene warm climate and annual primary productivity peaks recorded in sapropel deposition. Clim. Res. 31, 137–144.

Capozzi, R., Dinelli, E., Negri, A., Picotti, V., 2006b. Productivity-generated annual laminae in mid-Pliocene sapropels deposited during precessionally forced periods of warmer Mediterranean climate. Palaeogeogr. Palaeoclimatol. Palaeoecol. 235, 208–222.

Cardich, J., et al., 2015. Calcareous benthic foraminifera from the upper central Peruvian margin: control of the assemblage by pore water redox and sedimentary organic matter. Mar. Ecol. Prog. Ser. 535, 63–87.

Carmichael, M.J., et al., 2017. Hydrological and associated biogeochemical consequences of rapid global warming during the Paleocene-Eocene Thermal Maximum. Glob. Planet. Chang. 157, 114–138.

Carstensen, J., Conley, D.J., 2019. Baltic Sea hypoxia takes many shapes and sizes. Limnol. Oceanogr. Bull. 28, 125–129.

Carstensen, J., Andersen, J.H., Gustafsson, B.G., Conley, D.J., 2014. Deoxygenation of the Baltic Sea during the last century. PNAS 111, 5628–5633.

Casford, J.S.L., et al., 2002. Circulation changes and nutrient concentrations in the Late Quaternary Aegean Sea: a non-steady state concept for sapropel formation. Paleoceanogr. 17, 2000PA000601.

Castradori, D., 1993. Calcareous nannofossils and the origin of eastern Mediterranean sapropels. Paleoceanogr. 8, 459–471.

Ceballos, G., et al., 2015. Accelerated modern human–induced species losses: entering the sixth mass extinction. Sci. Adv. 1, e1400253.

Chen, Z.Q., Benton, M.J., 2012. The timing and pattern of biotic recovery following the end-Permian mass extinction. Nat. Geosci. 5, 375–383.

Chen, Z., et al., 2023. Freshwater ecosystem collapse and mass mortalities at the Paleocene-Eocene thermal maximum. Glob. Planet. Chang. 104175.

Conley, D.J., Björck, S., Bonsdorff, E., Carstensen, J., Destouni, G., et al., 2009. Hypoxia-related processes in the Baltic Sea. Environ. Sci. Technol. 43, 3412–3420.

Conley, D.J., et al., 2011. Hypoxia is increasing in the coastal zone of the Baltic Sea. Environ. Sci. Technol. 45, 6777–6783.

Corbí, H., Soria, J.M., Giannetti, A., Yébenes, A., 2020. The step-by-step restriction of the Mediterranean (start, amplification, and consolidation phases) preceding the Messinian Salinity Crisis (climax phase) in the Bajo Segura basin. Geo-Mar. Lett. 40, 341–361.

Cowie, R.H., Bouchet, P., Fontaine, B., 2022. The Sixth Mass Extinction: fact, fiction or speculation? Biol. Rev. 97, 640–663.

Crema, R., Castelli, A., Prevedelli, D., 1991. Long term eutrophication effects on macrofaunal communities in northern Adriatic Sea. Mar. Pollut. Bull. 22, 503–508.

Danovaro, R., 2018. Climate change impacts on the biota and on vulnerable habitats of the deep Mediterranean Sea. Rend. Linc. Sci. Fis. Nat. 29, 525–541.

De Lange, G.J., et al., 2008. Synchronous basin-wide formation and redox-controlled preservation of a Mediterranean sapropel. Nat. Geosci. 1, 606–610 (depletion at the onset of the Paleocene-Eocene Thermal Maximum as depicted in New).

Dera, G., et al., 2011. Climatic ups and downs in a disturbed Jurassic world. Geology 39, 215–218.

Diaz, R.J., Rosenberg, R., 2008. Spreading dead zones and consequences for marine ecosystems. Science 321, 926–929.

Doney, S.C., et al., 2012. Climate change impacts on marine ecosystems. Annu. Rev. Mar. Sci. 4, 11–37.

Eilola, K., Meier, H.M., Almroth, E., 2009. On the dynamics of oxygen, phosphorus and cyanobacteria in the Baltic Sea; a model study. J. Mar. Syst. 75, 163–184.

Elderbak, K., Leckie, R.M., Tibert, N.E., 2014. Paleoenvironmental and paleoceanographic changes across the Cenomanian–Turonian Boundary Event (Oceanic Anoxic Event 2) as indicated by foraminiferal assemblages from the eastern margin of the Cretaceous Western Interior Sea. Palaeogeogr. Palaeoclimatol. Palaeoecol. 413, 29–48.

Emeis, K.C., et al., 1996. Paleoceanography and sapropel introduction. In: Proceedings of the Ocean Drilling Program, Initial Reports, Vol. 160, pp. 21–28.

Emeis, K.C., Weissert, H., 2009. Tethyan–Mediterranean organic carbon-rich sediments from Mesozoic black shales to sapropels. Sedimentology 56, 247–266.

Emiliani, C., 1955. Pleistocene temperature variations in the Mediterranean. Quaternaria 3, 87–98.

Erba, E., 1994. Nannofossils and superplumes: the early Aptian "nannoconid crisis". Paleoceanogr. 9, 483–501.

Erba, E., 2004. Calcareous nannofossils and Mesozoic oceanic anoxic events. Mar. Micropaleontol. 52, 85–106.

Erba, E., Bottini, C., Weissert, H.J., Keller, C.E., 2010. Calcareous nannoplankton response to surface-water acidification around Oceanic Anoxic Event 1a. Science 329, 428–432.

Erba, E., Bottini, C., Faucher, G., Gambacorta, G., Visentin, S., 2019. The response of calcareous nannoplankton to Oceanic Anoxic events: the Italian pelagic record. Soc. Paleontol. Ital. 58, 51–71.

Ernst, R.E., Youbi, N., 2017. How large Igneous Provinces affect global climate, sometimes cause mass extinctions, and represent natural markers in the geological record. Palaeogeogr. Palaeoclimatol. Palaeoecol. 478, 30–52.

Filippelli, G.M., et al., 2003. A sediment–nutrient–oxygen feedback responsible for productivity variations in Late Miocene sapropel sequences of the western Mediterranean. Palaeogeogr. Palaeoclimatol. Palaeoecol. 190, 335–348.

Filippidi, A., De Lange, G.J., 2019. Eastern Mediterranean deep water formation during sapropel S1: a reconstruction using geochemical records along a bathymetric transect in the Adriatic outflow region. Paleoceanogr. Paleoclimatol. 34, 409–429.
Flecker, R., et al., 2015. Evolution of the Late Miocene Mediterranean–Atlantic gateways and their impact on regional and global environmental change. Earth Sci. Rev. 150, 365–392.
Foster, G.L., Royer, D.L., Lunt, D.J., 2017. Future climate forcing potentially without precedent in the last 420 million years. Nat. Commun. 8 (14845) https://doi.org/10.1038/ncomms14845.
Foster, G.L., Hull, P., Lunt, D.J., Zachos, J.C., 2018. Placing our current 'hyperthermal'in the context of rapid climate change in our geological past. Phil. Trans. R. Soc. A 376, 2130, 20170086.
Gerlach, T., 2011. Volcanic versus anthropogenic carbon dioxide. Eos, Trans. Amer. Geoph. Union 92, 201–202.
Giunta, S., Morigi, C., Negri, A., Guichard, F., Lericolais, G., 2007. Holocene biostratigraphy and paleoenvironmental changes in the Black Sea based on calcareous nannoplankton. Mar. Micropaleontol. 63, 91–110.
Glock, N., et al., 2019. Metabolic preference of nitrate over oxygen as an electron acceptor in foraminifera from the Peruvian oxygen minimum zone. PNAS 116, 2860–2865.
Gomi, Y., Fukuchi, M., Taniguchi, A., 2010. Diatom assemblages at subsurface chlorophyll maximum layer in the eastern Indian sector of the Southern Ocean in summer. J. Plan. Res 32, 1039–1050 (2010).
Gruber, N., 2011. Warming up, turning sour, losing breath: ocean biogeochemistry under global change. Phil. Trans. R. Soc. A 369, 1980–1996.
Handoh, I.C., Kawai, T., 2014. Modelling exposure of oceanic higher trophic-level consumers to polychlorinated biphenyls: pollution 'hotspots' in relation to mass mortality events of marine mammals. Mar. Pollut. Bull. 85, 824–830.
Handoh, I.C., Lenton, T.M., 2003. Periodic mid-Cretaceous oceanic anoxic events linked by oscillations of the phosphorus and oxygen biogeochemical cycles. Glob. Biogeochem. Cycles 17 (1092). https://doi.org/10.1029/2003GB002039.
Haywood, A.M., Sellwood, B.W., Valdes, P.J., 2000. Regional warming: Pliocene (3 Ma) paleoclimate of Europe and the Mediterranean. Geology 28, 1063–1066.
Haywood, A.M., et al., 2013. Large-scale features of Pliocene climate: results from the Pliocene Model Intercomparison Project. Clim. Past 9, 191–209.
He, T., Kemp, D.B., Li, J., Ruhl, M., 2023. Paleoenvironmental changes across the Mesozoic–Paleogene hyperthermal events. Glob. Planet. Chang. 104058 https://doi.org/10.1016/j.gloplacha.2023.104058.
Hedges, J.I., Keil, R.G., 1995. Sedimentary organic matter preservation: an assessment and speculative synthesis. Mar. Chem. 49, 81–115.
Hennekam, R., van der Bolt, B., van Nes, E.H., de Lange, G.J., Scheffer, M., Reichart, G.J., 2020. Early-warning signals for marine anoxic events. Geophys. Res. Lett. 47 e2020GL089183.
Hilgen, F.J., 1991. Astronomical calibration of Gauss to Matuyama sapropels in the Mediterranean and implication for the Geomagnetic Polarity Time Scale. Earth Planet. Sci. Lett. 107, 226–244.
Hilgen, F.J., et al., 1995. Extending the astronomical (polarity) time scale into the Miocene. Earth Planet. Sci. Lett. 136, 495–510.
Hu, X., Li, J., Han, Z., Li, Y., 2020. Two types of hyperthermal events in the Mesozoic-Cenozoic: Environmental impacts, biotic effects, and driving mechanisms. Sci. China Earth Sci. 63, 1041–1058.
Hu, R., Bostock, H.C., Gottschalk, J., Piotrowski, A.M., 2023. Reconstructing ocean oxygenation changes from U/Ca and U/Mn in foraminiferal coatings: proxy validation and constraints on glacial oxygenation changes. Quat. Sci. Rev. 306, 108028.
Huang, B., et al., 2017. Extended reconstructed sea surface temperature, version 5 (ERSSTv5): upgrades, validations, and intercomparisons. J. Clim. 30, 8179–8205.
Huang, J., et al., 2018. The global oxygen budget and its future projection. Sci. Bull. 63, 1180–1186.
IPCC, 2019. In: Pörtner, H.-O., Roberts, D.C., Masson-Delmotte, V., Zhai, P., Tignor, M., Poloczanska, E., Mintenbeck, K., Alegría, A., Nicolai, M., Okem, A., Petzold, J., Rama, B., Weyer, N.M. (Eds.), IPCC Special Report on the Ocean and Cryosphere in a Changing Climate.
Isozaki, Y., 1994. Superanoxia across the Permo-Triassic boundary: recorded in accreted deep-sea pelagic chert in Japan. Can. Soc. Petrol. Geol. Mem. 17, 805–812.
Isozaki, Y., 1997. Permo-Triassic boundary superanoxia and stratified superocean: records from lost deep sea. Science 276, 235–238.
Itaki, T., 2016. Transitional changes in microfossil assemblages in the Japan Sea from the Late Pliocene to Early Pleistocene related to global climatic and local tectonic events. Prog Earth Planet Sci 3, 11. https://doi.org/10.1186/s40645-016-0087-4.
Izumi, K., Endo, K., Kemp, D.B., Inui, M., 2018. Oceanic redox conditions through the late Pliensbachian to early Toarcian on the northwestern Panthalassa margin: Insights from pyrite and geochemical data. Palaeogeogr. Palaeoclimatol. Palaeoecol. 493, 1–10.
Jaraula, C.M., et al., 2013. Elevated pCO2 leading to Late Triassic extinction, persistent photic zone euxinia, and rising sea levels. Geology 41, 955–958.
Jenkyns, H.C., 2010. Geochemistry of oceanic anoxic events. Geochem. Geophys. Geosyst. 11 https://doi.org/10.1029/2009gc002788.
Jenkyns, H.C., 2018. Transient cooling episodes during Cretaceous Oceanic Anoxic Events with special reference to OAE 1a (Early Aptian). Phil. Trans. R. Soc. A 376, 20170073.
Joachimski, M.M., Alekseev, A.S., Grigoryan, A., Gatovsky, Y.A., 2020. Siberian Trap volcanism, global warming and the Permian-Triassic mass extinction: new insights from Armenian Permian-Triassic sections. GSA Bull. 132, 427–443.
Jones, M.M., et al., 2023. Abrupt episode of mid-Cretaceous ocean acidification triggered by massive volcanism. Nat. Geosci. 16, 169–174.
Jurikova, H., et al., 2020. Permian–Triassic mass extinction pulses driven by major marine carbon cycle perturbations. Nat. Geosci. 13, 745–750.
Karlson, B., et al., 2021. Harmful algal blooms and their effects in coastal seas of Northern Europe. Harmful Algae 102, 101989. https://doi.org/10.1016/j.hal.2021.101989.
Keeling, R.F., Körtzinger, A., Gruber, N., 2010. Ocean deoxygenation in a warming world. Annu. Rev. Mar. Sci. 2, 199–229.
Kemp, A.E., Villareal, T.A., 2013. High diatom production and export in stratified waters–a potential negative feedback to global warming. Prog. Oceanogr. 119, 4–23.
Kemp, A.E., Villareal, T.A., 2018. The case of the diatoms and the muddled mandalas: time to recognize diatom adaptations to stratified waters. Prog. Oceanogr. 167, 138–149.
Kemp, A.E.S., Pike, J., Pearce, R.B., Lange, C.B., 2000. The "Fall dump" — a new perspective on the role of a "shade flora" in the annual cycle of diatom production and export flux. Deep-Sea Res. II (47), 2129–2154.
Kemp, W.M., et al., 2005. Eutrophication of Chesapeake Bay: historical trends and ecological interactions. Mar. Ecol. Prog. Ser. 303, 1–29.
Knoll, A.H., Carroll, S.B., 1999. Early animal evolution: emerging views from comparative biology and geology. Science 284, 2129–2137.
Korte, C., et al., 2015. Jurassic climate mode governed by ocean gateway. Nat. Commun. 6 (10015) https://doi.org/10.1038/ncomms10015.
Kranner, M., Harzhauser, M., Beer, C., Auer, G., Piller, W.E., 2022. Calculating dissolved marine oxygen values based on an enhanced Benthic Foraminifera Oxygen Index. Sci. Rep. 12, 1376. https://doi.org/10.1038/s41598-022-05295-8.
Krause, A.J., et al., 2018. Stepwise oxygenation of the Paleozoic atmosphere. Nat. Commun. 9, 4081. https://doi.org/10.1038/s41467-018-06383-y.
Krueger, M.C., Harms, H., Schlosser, D., 2015. Prospects for microbiological solutions to environmental pollution with plastics. Appl. Microbiol. Biotechnol. 99, 8857–8874.
Kump, L.R., Pavlov, A., Arthur, M.A., 2005. Massive release of hydrogen sulfide to the surface ocean and atmosphere during intervals of oceanic anoxia. Geology 33, 397–400.
Kuypers, M.M., van Breugel, Y., Schouten, S., Erba, E., Damsté, J.S.S., 2004. N2-fixing cyanobacteria supplied nutrient N for cretaceous oceanic anoxic events. Geology 32, 853–856.
Kvale, K., Oschlies, A., 2023. Recovery from microplastic-induced marine deoxygenation may take centuries. Nat. Geosci. 16, 10–12.
Larson, R.L., Erba, E., 1999. Onset of the Mid-Cretaceous greenhouse in the Barremian-Aptian: Igneous events and the biological, sedimentary, and geochemical responses. Paleoceanogr. 14, 663–678.
Le Quéré, C., Andrew, R.M., Friedlingstein, P., Sitch, S., Pongratz, J., et al., 2018. Global carbon budget 2017. Ear. Sys. Scie. Data 10, 405–448.
Lear, C.H., et al., 2021. Geological Society of London Scientific Statement: what the geological record tells us about our present and future climate. J. Geol. Soc. 178 https://doi.org/10.1144/jgs2020-239.
Leckie, R.M., Bralower, T.J., Cashman, R., 2002. Oceanic anoxic events and plankton evolution: Biotic response to tectonic forcing during the mid-Cretaceous. Paleoceanography 17, 13–1.
Leipe, T., et al., 2011. Particulate organic carbon (POC) in surface sediments of the Baltic Sea. Geo-Mar. Lett. 31, 175–188.
Leipe, T., et al., 2017. Regional distribution patterns of chemical parameters in surface sediments of the south-western Baltic Sea and their possible causes. Geo-Mar. Lett. 37, 593–606.
Lenton, T.M., Daines, S.J., 2017. Biogeochemical transformations in the history of the ocean. Annu. Rev. Mar. Sci. 9, 31–58.
Li, M., Wignall, P.B., Dai, X., Hu, M., Song, H., 2021. Phanerozoic variation in dolomite abundance linked to oceanic anoxia. Geology 49, 698–702.
Limburg, K.E., Breitburg, D., Swaney, D.P., Jacinto, G., 2020. Ocean deoxygenation: a primer. One Earth 2, 24–29.
Lowery, C.M., et al., 2018. The late Cretaceous Western Interior Seaway as a model for oxygenation change in epicontinental restricted basins. Earth Sci. Rev. 177, 545–564.
Lowery, C.M., Bown, P.R., Fraass, A.J., Hull, P.M., 2020. Ecological response of plankton to environmental change: thresholds for extinction. Annu. Rev. Mar. Sci. 48, 403–429.
Mancini, A.M., et al., 2020. Calcareous nannofossil and foraminiferal trace element records in the Sorbas Basin: a new piece of the Messinian Salinity Crisis onset puzzle. Palaeogeogr. Palaeoclimatol. Palaeoecol. 554, 109796. https://doi.org/10.1016/j.palaeo.2020.109796.
Mancini, A.M., et al., 2023. Past Analogues of deoxygenation events in the Mediterranean Sea: a tool to constrain future impacts. J. Mar. Sci. Engi. 11, 562.
Marino, G., et al., 2007. Aegean Sea as driver of hydrographic and ecological changes in the eastern Mediterranean. Geology 35, 675–678.
Mattioli, E., Pittet, B., Petitpierre, L., Mailliot, S., 2009. Dramatic decrease of pelagic carbonate production by nannoplankton across the Early Toarcian anoxic event (T-OAE). Glob. Planet. Chang. 65, 134–145.
Mays, C., et al., 2021. Lethal microbial blooms delayed freshwater ecosystem recovery following the end-Permian extinction. Nat. Commun. 12, 5511.
Mee, L., 2006. Reviving dead zones. Sci. Am. 295, 78–85.
Meyer, K.M., Kump, L.R., 2008. Oceanic euxinia in Earth history: causes and consequences. Annu. Rev. Earth Planet. Sci. 36, 251–288.
Meyers, S.R., 2007. Production and preservation of organic matter: the significance of iron. Paleoceanography 22 (PA4211). https://doi.org/10.1029/2006PA001332.
Milkov, A.V., 2004. Global estimates of hydrate-bound gas in marine sediments: how much is really out there? Earth Sci. Rev. 66, 183–197.

Mojtahid, M., Manceau, R., Schiebel, R., Hennekam, R., de Lange, G.J., 2015. Thirteen thousand years of southeastern Mediterranean climate variability inferred from an integrative planktic foraminiferal-based approach. Paleoceanogr. 30, 402–422.
Mosch, T., et al., 2012. Factors influencing the distribution of epibenthic megafauna across the Peruvian oxygen minimum zone. Deep Sea Res. Part I Oceanogr. 68, 123–135.
Murat, A. Pliocene–Pleistocene occurrence of sapropels in the western Mediterranean Sea and their relation to eastern Mediterranean sapropels. In Proceedings of the Ocean Drilling Program (ed. Zahn, R., Comas, M.C., Klaus, A.). Scientific Results 161. Ocean Drilling Program, College Station, TX, pp. 519–527 (1999).
Naqvi, S.W.A., 2020. Ocean deoxygenation. Geol. Soc. Ind 96, 427–432.
Negri, A., 1996. Possible origin of laminated sediments of the anoxic Bannock Basin (eastern Mediterranean). Geo-Mar. Lett. 16, 101–107.
Negri, A., Wagner, T., Meyers, P.A., 2006. Introduction to“ Causes and consequences of organic carbon burial through time”. Palaeogeogr. Palaeoclimatol. Palaeoecol. 235, 1–7.
Nicolo, M.J., Dickens, G.R., Hollis, C.J., 2010. South Pacific intermediate water oxygen depletion at the onset of the Paleocene-Eocene thermal maximum as depicted in New Zealand margin sections. Paleoceanography 25, PA4210.
Nijenhuis, I.A., De Lange, G.J., 2000. Geochemical constraints on Pliocene sapropel formation in the eastern Mediterranean. Mar. Geol. 163, 41–63.
Nunes, F., Norris, R.D., 2006. Abrupt reversal in ocean overturning during the Palaeocene/Eocene warm period. Nature 439, 60–63.
Olausson, E., 1961. Studies of deep-sea cores. Reports of the Swedish Deep Sea Expedition. 1947-1948 (8), 353–391.
Oschlies, A., Brandt, P., Stramma, L., Schmidtko, S., 2018. Drivers and mechanisms of ocean deoxygenation. Nat. Geosci. 11, 467–473.
Parente, M., et al., 2008. Stepwise extinction of larger foraminifers at the Cenomanian-Turonian boundary: a shallow-water perspective on nutrient fluctuations during Oceanic Anoxic Event 2 (Bonarelli Event). Geology 36, 715–718.
Parker, F.L., 1958. Eastern mediterranean foraminifera. Reports of the Swedish deep-sea Expedition 8, 219–283.
Parslow, J.S., Boyd, P.W., Rintoul, S.R., Griffiths, F.B., 2001. A persistent subsurface chlorophyll maximum in the Interpolar Frontal Zone south of Australia: seasonal progression and implications for phytoplankton-light-nutrient interactions. J. Geoph. Res. Oc. 106, 31543–31557.
Pellegrino, L., Pierre, F.D., Natalicchio, M., Carnevale, G., 2018. The Messinian diatomite deposition in the Mediterranean region and its relationships to the global silica cycle. Earth Sci. Rev. 178, 154–176.
Pellegrino, L., et al., 2020. The upper Miocene diatomaceous sediments of the northernmost Mediterranean region: a lamina-scale investigation of an overlooked palaeoceanographic archive. Sedimentology 67, 3389–3421.
Penn, J.L., Deutsch, C., Payne, J.L., Sperling, E.A., 2018. Temperature-dependent hypoxia explains biogeography and severity of end-Permian marine mass extinction. Science 362, eaat1327. https://doi.org/10.1126/science.aat1327.
Penna, N., Capellacci, S., Ricci, F., 2004. The influence of the Po River discharge on phytoplankton bloom dynamics along the coastline of Pesaro (Italy) in the Adriatic Sea. Mar. Pollut. Bull. 48, 321–326.
Pérez-Asensio, J.N., et al., 2020. Changes in western Mediterranean thermohaline circulation in association with a deglacial Organic Rich Layer formation in the Alboran Sea. Quat. Sci. Rev. 228, 106075.
Perissoratis, C., Piper, D.J.W., 1992. Age, regional variation and shallowest occurence of S1 sapropel in the northern Aegean Sea. Geo-Mar. Lett. 12, 49–53.
Pierre, C., Belanger, P., Saliège, J.F., Urrutiaguer, M.J., Murat, A., 1999. Paleoceanography of the western Mediterranean during the Pleistocene oxygen and carbon isotope records at Site 975. In: Proceedings of the Ocean Drilling Program. Scientific Results, Vol. 161, pp. 481–488.
Pinardi, N., Masetti, E., 2000. Variability of the large-scale general circulation of the Mediterranean Sea from observations and modelling: a review. Palaeogeogr. Palaeoclimatol. Palaeoecol. 158, 153–173.
Pitcher, G.C., et al., 2021. System controls of coastal and open ocean oxygen depletion. Progr. Ocean. 197, 102613.
Pohl, A., et al., 2021. Vertical decoupling in Late Ordovician anoxia due to reorganization of ocean circulation. Nat. Geosci. 14, 868–873.
Powley, H.R., Van Krom, M.D., Cappellen, P., 2016. Circulation and oxygen cycling in the Mediterranean Sea: sensitivity to future climate change. J. Geophys. Res. Ocean. 121, 8230–8247.
Rabalais, N.N., Turner, R.E., Díaz, R.J., Justić, D., 2009. Global change and eutrophication of coastal waters. ICES J. Mar. Sci. 66, 1528–1537.
Rabalais, N.N., et al., 2010. Dynamics and distribution of natural and human-caused hypoxia. Biogeosciences 7, 585–619.
Rampino, M.R., Caldiera, K. & Prokoph, A., What causes mass extinctions? Large asteroid/comet impacts, flood-basalt volcanism, and ocean anoxia— In Correlations and Cycles, (ed. Koeberl, C., and Bice, D.M.) 250 Million Years of Earth History in Central Italy: Celebrating 25 Years of the Geological Observatory of Coldigioco: Geol. Soc. Am. Spec. 542, 1–32 (2019).
Raup, D.M., Sepkoski, J.J., 1982. Mass extinctions in the marine fossil record. Science 215, 1501–1503.
Reed, D.C., Slomp, C.P., Gustafsson, B.G., 2011. Sedimentary phosphorus dynamics and the evolution of bottom-water hypoxia: a coupled benthic–pelagic model of a coastal system. Limnol. Oceanogr. 56, 1075–1092.
Reershemius, T., Planavsky, N.J., 2021. What controls the duration and intensity of ocean anoxic events in the Paleozoic and the Mesozoic? Earth Sci. Rev. 221, 103787. https://doi.org/10.1016/j.earscirev.2021.103787.
Retallack, G.J., Jahren, A.H., 2008. Methane release from igneous intrusion of coal during late Permian extinction events. J. Geol. 116, 1–20.
Robert, C., Kennett, J.P., 1994. Antarctic subtropical humid episode at the Paleocene-Eocene boundary: clay-mineral evidence. Geology 22, 211–214.
Robinson, C., 2019. Microbial respiration, the engine of ocean deoxygenation. Front. Mar. Sci. 5, 533.
Rogerson, M., et al., 2008. A dynamic explanation for the origin of the western Mediterranean organic rich layers. Geochem. Geophys. Geosyst. 9, Q07U01. https://doi.org/10.1029/2007gc001936.
Rohling, E.J., 1994. Review and new aspects concerning the formation of Mediterranean sapropels. Mar. Geol. 122, 1–28.
Rohling, E.J., Bryden, H.L., 1992. Man-induced salinity and temperature increases in Western Mediterranean Deep Water. J. Geophys. Res. Atmos. 97, 11191–11198.
Rohling, E.J., Bryden, H.L., 1994. Estimating past changes in the eastern Mediterranean freshwater budget, using reconstructions of sea level and hydrography. Proc. K. Ned. Akad. Wet. Ser. B 97, 201–217.
Rohling, E.J., Gieskes, W.W.C., 1989. Late Quaternary changes in Mediterranean Intermediate Water density and formation rate. Paleoceanogr. 4, 531–545.
Rohling, E.J., Hilgen, F.J., 2007. The eastern Mediterranean climate at times of sapropel formation: a review. Neth. J. Geosci./Geol. En Mijnb. 70, 253–264.
Rohling, E.J., Marino, G., Grant, K.M., 2015. Mediterranean climate and oceanography, and the periodic development of anoxic events (sapropels). Earth Sci. Rev. 143, 62–97.
Roman, M.R., Brandt, S.B., Houde, E.D., Pierson, J.J., 2019. Interactive effects of hypoxia and temperature on coastal pelagic zooplankton and fish. Front. Mar. Sci. 6, 139.
Rose, K.A., et al., 2019. Impacts of ocean deoxygenation on ecosystem services: fisheries. In: Laffoley, D., Baxter, J.M. (Eds.), Ocean Deoxygenation: Everyone'S Problem - Causes, Impacts, Consequences and Solutions. IUCN, Gland, pp. 519–544.
Rossignol-Strick, M., 1983. African monsoons, an immediate climate response to orbital insolation. Nature 304, 46–49.
Rossignol-Strick, M., 1987. Rainy periods and bottom water stagnation initiating brine accumulation and metal concentrations: 1. The Late Quaternary. Paleoceanogr. 2, 333–360.
Rossignol-Strick, M., Paterne, M., 1999. A synthetic pollen record of the eastern Mediterranean sapropels of the last 1 Ma: implications for the time-scale and formation of sapropels. Mar. Geol. 153, 221–237.
Ruppel, C.D., Kessler, J.D., 2017. The interaction of climate change and methane hydrates. Rev. Geophys. 55, 126–168.
Sakalli, A., 2017. Sea surface temperature change in the Mediterranean Sea under climate change: a linear model for simulation of the sea surface temperature up to 2100. Appl. Ecol. Environ. Res. 15, 707–716.
Sanchez-Gomez, E., Somot, S., Déqué, M., 2009. Ability of an ensemble of regional climate models to reproduce weather regimes over Europe-Atlantic during the period 1961–2000. Clim. Dyn. 33, 723–736 sapropel in the northern Aegean Sea. Geomar. Lett. 12, 49–53 (1992).
Sarmiento, J.L., Gruber, N., 2006. Ocean Biogeochemical Dynamics. Princeton University Press.
Saunois, M., et al., 2020. The global methane budget 2000–2017. Earth Syst. Sci. Data 12, 1561–1623.
Schimmelmann, A., et al., 2016. Varves in marine sediments: a review. Earth Sci. Rev. 159, 215–246.
Schlitzer, 2011. Ocean Data View software. https://odv.awi.de accessed on 2 December 2022.
Schoepfer, S.D., Algeo, T.J., van de Schootbrugge, B., Whiteside, J.H., 2022. The Triassic–Jurassic transition–A review of environmental change at the dawn of modern life. Earth Sci. Rev. 104099 https://doi.org/10.1016/j.earscirev.2022.104099.
Scotese, C.R., 2021. An atlas of Phanerozoic paleogeographic maps: the seas come in and the seas go out. Annu. Rev. Earth Planet. Sci. 49, 679–728.
Scotese, C.R., Song, H., Mills, B.J., van der Meer, D.G., 2021. Phanerozoic paleotemperatures: the earth's changing climate during the last 540 million years. Earth Sci. Rev. 215, 103503.
Seliger, H.H., Boggs, J.A., Biggley, W.H., 1985. Catastrophic anoxia in the Chesapeake Bay in 1984. Science 228, 70–73.
Sherwood, S.C., et al., 2020. An assessment of Earth's climate sensitivity using multiple lines of evidence. Rev. Geophys. 58 e2019RG000678.
Sierro, F.J., et al., 2003. Orbitally-controlled oscillations in planktic communities and cyclic changes in western Mediterranean hydrography during the Messinian. Palaeogeogr. Palaeoclimatol. Palaeoecol. 190, 289–316.
Sluijs, A., et al., 2008. Arctic late Paleocene–early Eocene paleoenvironments with special emphasis on the Paleocene-Eocene thermal maximum (Lomonosov Ridge, Integrated Ocean Drilling Program Expedition 302). Paleoceanography 23, PA4216. https://doi.org/10.1029/2008PA001615.
Smith, J.L.L., Oseid, D.M., Kimball, G.L., El-Kandelgy, S.M., 1976. Toxicity of hydrogen sulfide to various life history stages of bluegill (*Lepomis macrochirus*). Trans. Am. Fish. Soc. 105, 442–449.
Somot, S., Sevault, F., Déqué, M., 2006. Transient climate change scenario simulation of the Mediterranean Sea for the twenty-first century using a high-resolution ocean circulation model. Clim. Dyn. 27, 851–879.
Sondi, I., Juračić, M., 2010. Whiting events and the formation of aragonite in Mediterranean Karstic Marine Lakes: new evidence on its biologically induced inorganic origin. Sedimentology 57, 85–95.
Song, H., et al., 2014. Anoxia/high temperature double whammy during the Permian-Triassic marine crisis and its aftermath. Sci. Rep. 4, 4132.
Song, H., et al., 2017. The onset of widespread marine red beds and the evolution of ferruginous oceans. Nat. Commun. 8 https://doi.org/10.1038/s41467-017-00502-x.
Song, H., Wignall, P.B., Dunhill, A.M., 2018. Decoupled taxonomic and ecological recoveries from the Permo-Triassic extinction. Sci. Adv. 4 https://doi.org/10.1126/

sciadv.aat5091 eaat5091. (special emphasis on the Paleocene-Eocene thermal maximum (Lomonosov Ridge).
Song, H., et al., 2019. Seawater temperature and dissolved oxygen over the past 500 million years. J. Ear. Sci. 30, 236–243.
Song, H., et al., 2021. Thresholds of temperature change for mass extinctions. Nat. Commun. 12, 4694. https://doi.org/10.1038/s41467-021-25019-2.
Speijer, R.P., Wagner, T., 2002. Sea-level changes and black shales associated with the late Paleocene thermal maximum: organic-geochemical and micropaleontologic evidence from the southern Tethyan margin (Egypt-Israel). Special Papers-Geological Society of America 533-550.
Sperling, M., et al., 2003. Black Sea impact on the formation of eastern Mediterranean sapropel S1? Evidence from the Marmara Sea. Palaeogeogr. Palaeoclimatol. Palaeoecol. 190, 9–21.
Stachowitsch, M., 1984. Mass mortality in the Gulf of Trieste: the course of community destruction. Mar. Ecol. 5, 243–264.
Stachowitsch, M., Riedel, B., Zuschin, M., 2012. The return of shallow shelf seas as extreme environments: Anoxia and Macrofauna Reactions in the Northern Adriatic Sea. In: Altenbach, A.V. (Ed.), Anoxia: Evidence for Eukaryote Survival and Paleontological Strategies. Springer, pp. 353–368.
Steckbauer, A., Duarte, C.M., Carstensen, J., Vaquer-Sunyer, R., Conley, D.J., 2011. Ecosystem impacts of hypoxia: thresholds of hypoxia and pathways to recovery. Environ. Res. Lett. 6, 025003 https://doi.org/10.1088/1748-9326/6/2/025003.
Steuber, T., Löser, H., Mutterlose, J., Parente, M., 2023. Biogeodynamics of Cretaceous marine carbonate production. Earth Sci. Rev. 104341, 1016/j.earscirev.2023.104341.
Stramma, L., Johnson, G.C., Sprintall, J., Mohrholz, V., 2008. Expanding oxygen-minimum zones in the tropical oceans. Science 320, 655–658.
Sun, Y., et al., 2012. Lethally hot temperatures during the Early Triassic greenhouse. Science 338, 366–370.
Tada, R., Irino, T., Koizumi, I., 1999. Land–ocean linkages over orbital and millennial timescales recorded in late Quaternary sediments of the Japan Sea. Paleoceanogr. 14, 236–247.
Tada, R., Murray, R.W., Alvarez Zarikian, C.A., 2015. the Expedition 346 Scientists. Proceedings of Integrated Ocean Drilling Program. IODP, vol 346. Integrated Ocean Drilling Program, College Station. https://doi.org/10.2204/iodp.proc.346.101.
Tada, R., et al., 2018. High-resolution and high-precision correlation of dark and light layers in the Quaternary hemipelagic sediments of the Japan Sea recovered during IODP Expedition 346. Progr. Ear. Plan. Sci. 5, 1–10.
Takashima, R., Nishi, H., Huber, B.T., Leckie, R.M., 2006. Greenhouse world and the Mesozoic Ocean. Oceanogr. 19, 82–93.
Talley, L.D., et al., 2006. Japan/East Sea water masses and their relation to the sea's circulation. Oceanogr. 19, 32–49.
Taylforth, J.E., et al., 2014. Middle Miocene (Langhian) sapropel formation in the easternmost Mediterranean deep-water basin: evidence from northern Cyprus. Mar. Pet. Geol. 57, 521–536.
Tebaldi, C., et al., 2020. Climate model projections from the scenario model intercomparison project (ScenarioMIP) of CMIP6. Earth Syst. Dyn. Discuss 2020, 1–50.
Thomas, E., Shackleton, N.J., 1996. The Paleocene-Eocene benthic foraminiferal extinction and stable isotope anomalies. Geol. Soc. London Spec. Pub. 101, 401–441.
Tréguer, P., et al., 2018. Influence of diatom diversity on the ocean biological carbon pump. Nat. Geosci. 11, 27–37.
Tremolada, F., De Bernardi, B., Erba, E., 2008. Size variations of the calcareous nannofossil taxon *Discoaster multiradiatus* (Incertae sedis) across the Paleocene–Eocene thermal maximum in ocean drilling program holes 690B and 1209B. Mar. Micropaleontol. 67, 239–254.
Tyrrell, T., 1999. The relative influences of nitrogen and phosphorus on oceanic primary production. Nature 400, 525–531.
Tyson, R.V., Pearson, T.H., 1991. Modern and ancient continental shelf anoxia: an overview. Geol. Soc. Lond. Spec. Publ. 58, 1–24.
Van Cappellen, P., Ingall, E.D., 1994. Benthic phosphorus regeneration, net primary production, and ocean anoxia: a model of the coupled marine biogeochemical cycles of carbon and phosphorus. Paleocean. 9, 677–692.
van de Schootbrugge, B., et al., 2007. End-Triassic calcification crisis and blooms of organic-walled 'disaster species'. Palaeogeogr. Palaeoclimatol. Palaeoecol. 244, 126–141.
Viktorsson, L., Ekeroth, N., Nilsson, M., Kononets, M., Hall, P.O.J., 2013. Phosphorus recycling in sediments of the central Baltic Sea. Biogeosciences 10, 3901–3916.
von Grafenstein, R., et al. Planktonic δ18O records at Sites 976 and 977, Alboran Sea: stratigraphy, forcing, and paleoceanographic implications. Proceedings ODP, Scientific Results, (ed. Zahn, R., Comas, MC, and Klaus, A.) Ocean Drilling Program, College Station, TX, 469–479 (1999).
Von Westernhagen, H., Dethlefsen, V., 1982. Effect of the surfactant Corexit 7664 on uptake of cadmium by organisms and biological matter in a closed circulated brackish-water system. Helg. Meeresunt. 35, 1–12.
Watanabe, S., Tada, R., Ikehara, K., Fujine, K., 2007. Kido Y Sediment fabrics, oxygenation history, and circulation modes of Japan Sea during the Late Quaternary. Palaeogeogr. Palaeoclimatol. Palaeoecol. 247, 50–64.
Watson, A.J., Lenton, T.M., Mills, B.J., 2017. Ocean deoxygenation, the global phosphorus cycle and the possibility of human-caused large-scale ocean anoxia. Phil. Trans. R. Soc. A 375, 2102, 20160318.
Weldeab, S., Menke, V., Schmiedl, G., 2014. The pace of East African monsoon evolution during the Holocene. Geophys. Res. Lett. 41, 1724–1732.
Westman, P., Sohlenius, G., 1999. Diatom stratigraphy in five offshore sediment cores from the northwestern Baltic proper implying large scale circulation changes during the last 8500 years. J. Paleolimn. 22, 53–69.
Wignall, P.B., Hallam, A., 1992. Anoxia as a cause of the Permian/Triassic mass extinction: Facies evidence from northern Italy and the western United States. Palaeogeogr. Palaeoclimatol. Palaeoecol. 93, 21–46.
Wignall, P.B., Twitchett, R.J., 1996. Oceanic anoxia and the end Permian mass extinction. Science 272, 1155–1158.
Wu, Y., et al., 2021. Six-fold increase of atmospheric p CO2 during the Permian–Triassic mass extinction. Nat. Commun. 12, 2137.
Wu, Y., Cui, Y., Chu, D., Song, H., Tong, J., Dal Corso, J., Ridgwell, A., 2023. Volcanic CO2 degassing postdates thermogenic carbon emission during the end-Permian mass extinction. Sci. Adv. 9, eabq4082.
Wunsam, S., Schmidt, R., Müller, J., 1999. Holocene lake development of two Dalmatian lagoons (Malo and Veliko Jezero, Isle of Mljet) in respect to changes in Adriatic sea level and climate. Palaeogeogr. Palaeoclimatol. Palaeoecol. 146, 251–281.
Yao, W., Paytan, A., Wortmann, U.G., 2018. Large-scale ocean deoxygenation during the Paleocene-Eocene Thermal Maximum. Science 361, 804–806.
Yasuhara, M., Tittensor, D.P., Hillebrand, H., Worm, B., 2017. Combining marine macroecology and palaeoecology in understanding biodiversity: microfossils as a model. Biol. Rev. 9, 199–215.
Yasuhara, M., Rabalais, N.N., Conley, D.J., Gutierrez, D., 2019. Palaeo-records of histories of deoxygenation and its ecosystem impact. Ocean deoxygenation: Everyone's problem. https://doi.org/10.2305/iucn.ch.2019.14.en.
Zachos, J.C., et al., 2005. Rapid acidification of the ocean during the Paleocene-Eocene thermal maximum. Science 308, 1611–1615.
Zeebe, R.E., Ridgwell, A., Zachos, J.C., 2016. Anthropogenic carbon release rate unprecedented during the past 66 million years. Nat. Geosci. 9, 325–329.

Further-reading

Hallam, A., Wignall, P.B., 1997. Mass Extinctions and their Aftermath. Oxford University Press, UK.